

MODELLING OF WEDGE WATER ENTRY PROBLEM BY SPH METHOD

YILDIZ EKŞİ

M.Sc. THESIS

2019



YILDIZ EKŞİ

PÎRÎ REİS UNIVERSITY

2019

MODELLING OF WEDGE WATER ENTRY PROBLEM BY SPH METHOD

by

Yıldız Ekşi

B. Sc., Mathematics, Uludag University, 2007

B. Sc., Naval Architecture and Marine Engineering, Piri Reis University, 2016

Submitted to the Institute for Graduate Studies in
Science and Engineering in partial fulfillment of
the requirements for the degree of
Master of Science

Graduate Program in Naval Architecture and Marine Engineering
High Performance Ocean Platforms
Piri Reis University
2019

MODELLING OF WEDGE WATER ENTRY PROBLEM
BY SPH METHOD


APPROVED BY:

Asst. Prof. Murat Özbek
(Thesis Supervisor)



.....

Asst. Prof. A. Ziya Saydam



.....

Prof. Ömer Gören



.....

DATE OF APPROVAL:09.08.2019.....



To my family,

“Dinlenmemek üzere yürümeye karar verenler, asla ve asla yorulmazlar. Türk gençliği gayeye, bizim yüksek idealimizle durmadan, yorulmadan yürüyeceklerdir.”

(Those who decided to walk and not to get rest would never get tired. Turkish youth which is together with our high ideal would walk towards the aim without stopping or getting tired.)

Mustafa Kemal Atatürk

ACKNOWLEDGEMENTS

I would like to express my eternal thanks to the following persons for their continued support and understanding during the thesis research and compilation of this study.

Asst. Prof. Murat Özbulut, for his teaching, enormous patience, continuous support and guiding through all steps of my thesis research.

Prof. Sander Çalışal for encouragements, advice, professional guidance, and enlightening me with his vision.

Prof. Mehmet Yıldız for his teaching and support.

Asst. Prof. Serhan Gökçay, for his support and understanding.

Asst. Prof. A. Ziya Saydam, for his support, understanding and serving on my committee.

Prof. Ömer Gören, for serving on my committee.

TUBITAK for financial support provided by the Scientific and Technological Research Council of Turkey for project number 117M091.

My friends, for their support, understanding and their time that they spent for me.

Çağdaş Akalın, for his continuous support, encouragement and being more than a friend.

Finally, **My family**, for their priceless support, encouragement and always standing my behind at all stages of my life.

Yıldız Ekşi

TABLE OF CONTENTS

ACKNOWLEDGEMENTS	vi
ABBREVIATIONS	ix
LIST OF TABLES	x
LIST OF FIGURES	xi
LIST OF SYMBOLS	xiii
ABSTRACT	xiv
ÖZET	xvi
1 INTRODUCTION	1
1.1 Motivation	1
1.2 Objectives of the Thesis	2
1.3 Outline of the Thesis	4
2 BACKGROUND	7
2.1 Lagrangian and Eulerian Descriptions of Particle Motion	7
2.2 Literature Review	8
2.2.1 Introduction	8
2.2.2 Meshfree Methods	9
2.2.3 Smoothed Particle Hydrodynamics	10
2.2.4 Overview of Water Entry Problem	13
3 SMOOTHED PARTICLE HYDRODYNAMICS	19
3.1 Integral Representation of a Function in SPH Method	19
3.2 Particle Approximation	21
3.3 Application of Particle Approximation to Governing Equations	22
3.4 Weight (Kernel) Functions in SPH Methods	26
3.5 Mathematical Modelling	30
3.5.1 Governing Equations	30
3.5.2 SPH Approximation and Discretization of Momentum Equations	32
3.6 Corrective Numerical Algorithms	33
3.6.1 Gradient Correction of Weight Function	33
3.6.2 Density Correction	34
3.6.3 Free Surface Correction	34
3.6.4 Particle Displacement Correction	35
3.7 Time Integration and Boundary Conditions	36

4	SPH MODELLING OF WEDGE ENTRY PROBLEM WITH CONSTANT VELOCITY AND ACCELERATION	39
4.1	Problem Geometry and Parameters	39
4.2	Numerical Results of Constant Velocity	41
4.3	Viscous Penalty Treatment in SPH Scheme	43
4.3.1	SPH Results with Viscous Penalty Method	49
4.4	Numerical Results of Constant Acceleration	49
5	SPH MODELING OF WEDGE ENTRY PROBLEM WITH FREE FALL	55
5.1	Problem Geometry and Parameters	55
5.1.1	Fluid–Solid Interaction Algorithm	55
5.2	Numerical Results	57
6	CONCLUDING REMARKS	63
	REFERENCES	65

ABBREVIATIONS

CFD	C omputational F luid D ynamics
CSPH	C orrective S moothed P article H ydrodynamics
CSPM	C orrective S moothed P article M ethods
DPD	D issipative P article D ynamics
DSPH	D iscontinous S moothed P article H ydrodynamics
ISPH	I ncompressible S moothed P article H ydrodynamics
FDM	F inite D ifference M ethods
FEM	F inite E lement M ethod
FPM	F inite P article M ethods
FSI	F luid S olid I nteraction
FVM	F inite V olume M ethods
GSM	G radient S moothing M ethod
MD	M olecular D ynamics
MLSPH	M oving L east S moothed P article H ydrodynamics
MSPH	M odified S moothed P article H ydrodynamics
ODE	O rdinary D ifferential E quation
PDE	P artial D ifferential E quation
RKPM	R eproducing K ernel P article M ethod
SPH	S moothed P article H ydrodynamics
VOF	V olume O f F luid
VP	V iscous P enalty
WCSPH	W eakly C ompressible S moothed P article H ydrodynamics
WHM	W eighted H armonic M ean

LIST OF TABLES

Table 4.1 Computational time cost per unit cycle for variable initial particle spacing	42
--	----



LIST OF FIGURES

Figure 3.1	Visual representation of a Kernel function,[32]	26
Figure 3.2	The function of Gaussian kernel and its derivative	28
Figure 3.3	The function of cubic kernel and its derivative	29
Figure 3.4	The function of cubic kernel and its derivative	30
Figure 4.1	Schematic representation of problem geometry	39
Figure 4.2	Schematic representation of problem geometry	40
Figure 4.3	Representation of pressure points on the wedge	40
Figure 4.4	Falling sequence	42
Figure 4.5	35 degree, t=0.073s, delta=6mm	43
Figure 4.6	35 degree, t=0.079s, delta=8mm	44
Figure 4.7	35 degree, t=0.085s, delta=10mm	45
Figure 4.8	35 degree, t=0.085s, delta=10mm, h=2mm	46
Figure 4.9	30 degree, t=0.085s, delta=10mm, h=1.33mm	47
Figure 4.10	30 degree, t=0.070s, delta=10mm, h=1.6mm	48
Figure 4.11	Comparison of pressure distribution	49
Figure 4.12	Comparison of pressure distribution with VP method	50
Figure 4.13	SPH method vs VP method (6mm)	50
Figure 4.14	SPH method vs VP method (8mm)	51
Figure 4.15	SPH method vs VP method (10mm)	51
Figure 4.16	Change in displacement, the velocity of the wedge body and pressure values captured from sensor points for 10mm delta distance with constant acceleration	52
Figure 4.17	Change in displacement, the velocity of the wedge body and pressure values captured from sensor points for 10mm delta distance with constant acceleration-a close-up view after the moment of impact .	52
Figure 4.18	Change in displacement, the velocity of the wedge body and pressure values captured from sensor points for 6mm delta distance with constant acceleration	53
Figure 4.19	Change in displacement, the velocity of the wedge body and pressure values captured from sensor points for 6mm delta distance with constant acceleration-a close-up view after the moment of impact . . .	54
Figure 5.1	Schematic representation of problem geometry	56
Figure 5.2	Change in displacement, the velocity of the wedge body and pressure values captured from sensor points for 35.6° deadrise angle, H=1.0m, a=0.324m	58
Figure 5.3	Change in displacement, the velocity of the wedge body and pressure values captured from sensor points for 37.3° deadrise angle, H=1.0m, a=0.334m	59

Figure 5.4	Change in displacement, the velocity of the wedge body and pressure values captured from sensor points for 37.3° deadrise angle, $H=0.5\text{m}$, $a=0.334\text{m}$	59
Figure 5.5	Change in displacement, the velocity of the wedge body and pressure values captured from sensor points for 37.3° deadrise angle, $H=0.5\text{m}$, $a=0.324\text{m}$	60
Figure 5.6	Change in displacement, the velocity of the wedge body and pressure values captured from sensor points for 36.8° deadrise angle, $H=0.5\text{m}$, $a=0.324\text{m}$	61
Figure 5.7	Change in displacement, the velocity of the wedge body and pressure values captured from sensor points for 37° deadrise angle, $H=0.5\text{m}$, $a=0.324\text{m}$	61



LIST OF SYMBOLS

c_0	speed of sound
d^3r_{ij}	infinitesimal volume element
h	smoothing length
i	(i index) indicates the particle interested
j	(j index) other particles which interact with the particle i
m_j	mass of particle j
P	pressure
r_i	position of particle i
r_{ij}	the distance vector between two particles
R	relative distance between two particles
\vec{u}	particles velocity vector
ν	kinematic viscosity
V	volume
W, W_{ij}	kernel, weighting function
x_i	position vector
α_d	space (2-D)
γ	specific heat ratio of water (7)
δ	Kronecker-Delta operator
ρ	density of particles
$\hat{\rho}_i$	density correction
Ω	the volume of interaction region
∇	gradient
$\langle \rangle$	kernel approximation operator

ABSTRACT

MODELLING OF WEDGE WATER ENTRY PROBLEM BY SPH METHOD

Due to its importance in many practical applications in ship hydrodynamics and ocean engineering, the water entry problem is a challenging problem due to the modeling of instantaneous high pressures that occur during a collision of any arbitrary body to the fluid medium.

Specifically, understanding of the physical phenomenon that occurs during the motion of a ship body provides useful information for optimization for structural endurance and motion stability. Numerical techniques enable us to obtain significant outcomes based on their theoretical background which is used to define the physical problem mathematically.

During its motion in severe service conditions, a ship body is exposed to extreme and sudden pressure changes on its external shell structure causing impact loadings. In this manner, wedge entry phenomenon that may cause damaging impacts is because of fluid-solid interaction and shall be regarded as extremely important since its investigation provides useful information for the structural design and predicting endurance of the hull geometry. Numerical methods to solve mathematical models for such phenomena can provide quantitative outcomes for pressure distribution over the region where fluid-solid interaction occurs.

As an engineering approach, the cross-section of a ship body in two-dimension is geometrically approximated as a wedge and pressure distribution along the edges is investigated for various collision scenarios.

Developments in the computational technology have provided faster computations and accelerated the to obtain numerical results. In time, computational power has spread in science and technology as well as in computational implementations of Smoothed Particle Hydrodynamics.

The aim of this thesis study is to model the problem of access to the element numerically by using the Lagrangian particle based sph method. In this scope, a two-dimensional SPH algorithm was developed and a triangular body was first modeled at a constant speed to the calm water surface. The pressure distributions on the surface of the triangular body are calculated at the given sensor points of the experimental/numerical measurements in the literature.

Furthermore, additional treatments which are known as viscous penalty method and fluid-solid interaction are coupled with weakly compressible smoothed particle hydrodynamics method and obtained numerical results are correlated with reference studies.

Keywords: SPH method, Wedge entry, Water entry, CFD modelling, Free-falling object, Free solid body-fluid interactions

ÖZET

ÜÇGEN CİSMİN SUYA GİRİŞ PROBLEMİNİN İPH METODU İLE MODELLENMESİ

Gemi hidrodinamiği ve okyanus mühendisliği gibi, birçok pratik uygulamadaki önemi nedeniyle, matematik ve mühendislik bilim insanları tarafından dikkat çeken suya giriş problemi, çarpışma anında açığa çıkan yüksek basınçların modellenmesi dolayısıyla önemli bir problemdir.

Spesifik olarak, bir gemi gövdesinin hareketi sırasında meydana gelen fiziksel olgunun anlaşılması, gövde geometrisinin optimizasyonu, enerji verimliliğinin ve hareket stabilitesinin artırılması için yararlı bilgiler sağlar. Sayısal teknikler, fiziksel problemi matematiksel olarak tanımlamak için kullanılan teorik arka planına dayanarak önemli sonuçlar elde etmemizi sağlar.

Bir geminin şiddetli deniz koşullarında seyrederken, gemi gövdesi aşırı ve ani basınç değişiklikleri nedeniyle oluşan darbe yüklerine maruz kalır. Bu bağlamda, hasara sebebiyet verebilecek olan suya giriş olayı katı-sıvı fazlarının etkileşimi ile ilişkilidir. Gemi gövdesi üzerinde şiddetli hasarlara sebep olabilecek bu problemin incelenmesi, yapısal tasarım ve gemi gövdesinin dayanıklılığının öngörülebilmesi için önemlidir. Bu tür olayların incelenmesi, akışkan-katı etkileşimin gerçekleştiği bölge üzerinde matematiksel modelleri çözmek için kullanılan sayısal yöntemlerin kullanılması gemi gövdesi üzerindeki basınç dağılımı için nicel sonuçlar sağlayabilir.

Bir gemi gövdesinin kesiti belirli bir yaklaşıklıkla bir üçgen geometrisinin sınırları olarak değerlendirilebilir ve üçgenin kenarları boyunca basınç dağılımı çeşitli çarpışma senaryoları için incelenebilir.

Geçtiğimiz on yıl boyunca, elektronik cihazların hesaplama kapasitesindeki gelişmeler bilgisayarlardan nümerik sonuçlar elde etmede etkinliğini arttırmıştır. Zaman içinde, hesaplama gücü bilimde ve teknolojide olduğu gibi İnterpolasyonlu Parçacık Hidrodinamiğinin hesaplamalı uygulamalarında da yaygın olarak kullanılmaya başlamıştır.

Bu tez çalışması suya giriş probleminin Lagrangian parçacık tabanlı olan SPH metodu kullanılarak nümerik olarak modellenmesini hedeflemektedir. Bu kapsamda, iki boyutlu SPH algoritması geliştirilmiş ve ilk olarak sakin su yüzeyine sabit hızda çarpan ve hareketine sabit hızla devam etmeye zorlanan bir üçgen kesitli cisim üzerinde kullanılmıştır. Üçgen gövdenin yüzeyindeki basınç dağılımları, literatürdeki benzer sayısal/deneysel çalışmalarda gösterilen sensör noktaları üzerinden hesaplanmıştır.

Ayrıca, viskoz penaltı yöntemi ve katı-sıvı etkileşimi olarak bilinen iyileştirmeler, zayıf sıkıştırılabilir parçacık hidrodinamiği yöntemi ile birleştirilmiş ve elde edilen sayısal sonuçlar referans çalışmaları ile ilişkilendirilmiştir.

Anahtar Kelimeler: İnterpolasyonlu parçacık hidrodinamiği (İPH), Üçgen cismin suya giriş problemi, Hesaplamalı Akışkanlar Dinamiği (HAD) ile modelleme, Serbest düşme, Serbest katı cisim-akışkan etkileşimleri

1. INTRODUCTION

1.1 Motivation

Nowadays, many numerical methods based on different discretization approaches are used extensively in solving engineering problems. However, the selection of appropriate numerical techniques depending on the problem such as wedge entry phenomenon is extremely essential since mesh-based models are not capable of capturing high deformations. Thus, in this thesis study, the SPH method, being a particle-based approach is used to solve the water entry problem of a wedge body for numerical investigation of the pressure field in the liquid domain.

Compared to mesh-based numerical methods, the particle base methods are more capable of capturing severe deformations with no need to remesh the material domain. Mesh generation of complex geometries and resolving free-surface boundaries require more computational time needed compared to mesh-free particle methods.

In addition, these numerical methods are quite important in terms of providing an alternative solution to the situations in case performing experiments is not possible. Moreover, numerical models may need to be validated in terms of their robustness in the sense of how much they are consistent with experimental results. Most of the time, exact solutions for computational problems are not easy to handle and also suitable numerical methods provide a powerful alternative way to obtain exact solutions. By means of discretization techniques, it becomes convenient to convert continues forms of governing equations in integral or differential representations into the discrete state. Furthermore, the implementation part of the discrete forms of governing equations into a computer program in a programming language is needed to solve the equations numerically and obtain desired results. The SPH method is a computational approach for flow motion simulation of liquid media based on theoretical construction behind it. Analysis of flow motion in the SPH method provides quantitative results regarding hydrodynamic parameters e.g. pressure, force, velocity fields of the liquid medium under consideration.

In addition to other reliable numerical techniques, the SPH method arises as an alternative investigation against hands-on studies which are in most cases extreme efforts in terms of time and money. In many small scale experimental studies, however, they can be regarded as computational power to make a correlation for real-life engineering problems based on theoretical approaches. The SPH method is used for the high-speed event and extreme deformations. Some examples where SPH has been studied include a splash of water, sloshing, fluid interaction with solid structure, ballistics, spraying, gas flow. And to give some examples for marine areas, free-falling lifeboat simulation, wave engineering, and slamming motion can be given.

While a ship is traveling in rough seas, slamming motion produces high magnitude pressure impact in very short time duration, especially, between the bow of the ship and the water surface.

All in all, after considering all the advantages of particle-based methods for the investigation of hydrodynamic impacts during solid-fluid interactions, the SPH method was implemented to the wedge entry phenomenon in a two-dimensional problem domain.

1.2 Objectives of the Thesis

In this recent thesis study, a numerical two-dimensional wedge water entry model is developed by the SPH method. Handling moving boundary conditions for wedge water entry problems by means of mesh-based numerical methods may cause complex calculations compared to the SPH method. The reason for that the SPH method is preferred to use in the wedge water entry problem to capture the extreme pressure jump occurs at the collusion instant. This phenomenon may cause difficulty in terms of capturing the pressure values along the edge of the wedge geometry. As to be able to capture the high free surface deformations in this region, there is often a re-meshing of the network system with complex algorithms.

Particularly in recent years, intensive research has been carried out on particle methods in order to contribute to overcome the difficulty experienced in conventional

mesh-based methods in the modeling of free water surface fluid flow problems. As opposed to that, high deformations on the free water surface can be easily modeled by means of the SPH method compared to mesh-based numerical approaches due to its advantage in solving the equations of motion in the discrete state.

The main objective of this thesis study is to contribute to the literature with an investigation of high-velocity impact modeling of a rigid body to free surface problems. For this aim, the SPH method is used in numerical calculations. Because of its particle-based nature of the method, fluid motion is defined by the Lagrange approach, and thus the non-linear convective derivative term in the material derivative expression is eliminated.

In the current literature, there are two distinct approaches in the context of SPH whose formulations are structured depending on the way that the pressure term in the equation of motion is computed.

In the incompressible SPH (ISPH) method, the rigid body motion together with the viscous penalty which is required for inducing rigidly is used to simulate rigid body motion. The equation of motion includes a pressure term. In relation to this, Cummins et. al proposed an approach based on the projection method where the pressure Poisson equation is used to calculate this pressure term [26].

Implementing weakly compressible SPH (WCSPH) requires subtle treatment of its various components. For instance, an artificial equation of state which enables coupling between density and pressure by means of speed of sound which is necessary to provide incompressibility. All fluids can be considered as compressible to some degree. In relation to this, weakly compressibility of fluid is associated with small dilatations and causes a change in the density of the fluid, leading to significant variation in pressure. Therefore, the application of corrective numerical treatments such as density filtering becomes necessary to alleviate oscillation in the pressure field, and numerical stability which often dictates small time steps [57, 90].

Beside, problems, where fluid-solid interaction is coupled with the SPH method,

have been studied in the literature. In these SPH studies which are rare but significant include investigation of solid body motion of the particles inside liquid mediums. WCSPH has also been applied as a method for the solid particles' motion inside the liquid medium [47, 71]. For instance, the sedimentation problem of solid particles by means of a modified boundary condition was studied by Hashemi et al. [46]. Another application of the WCSPH method by Bian et al. [15] has been implemented to present a model for suspension liquids containing concentrated particles. The studies in the field have been shown that flow motion of coupled fields can be improved in terms of results, governing equations used and numerical implementation of formulations.

1.3 Outline of the Thesis

After a brief introduction to the objective of this thesis study, in the following sections, theoretical background, numerical implementation schemes of the governing formulations are introduced and numerical outcomes are discussed based on benchmark studies in the literature.

In more detail, a wide variety of numerical methods previously studied in particle descriptions, SPH method, and wedge entry problem have been extensively reviewed in Chapter (2).

In Chapter (3), the basic idea of the SPH method and its fundamental formulations are introduced with distinct prescriptions of terms appearing in the equations. Its integral representation of smoothing function in the SPH method is explained and the continuous integral representation (kernel approximation) and the discretized particle approximation and their application to the governing equations are given in Chapter (3) as well. Explanation of the correction algorithms applied to the governing equation in the numerical code is given in the same chapter of the study.

Definition for the wedge entry problem with constant velocity and acceleration is introduced in Chapter (4) in detail and then the geometry for the problem and other related parameters are clearly defined. Hereby, the numerical results related to the problem defined are presented.

Chapter (5) presents SPH modeling of wedge entry problem with free fall and comparison of the results with numerical findings in the literature.

Significant outcomes from Chapters (4) and 5) are provided in Chapter (6). Also, general remarks and recommendations for future studies were summarized here as well.



2. BACKGROUND

In this chapter, general information about the SPH method and wedge entry, and their historical background is given.

2.1 Lagrangian and Eulerian Descriptions of Particle Motion

The SPH method uses Lagrangian formulation for analysis of the deformation field in material domain where interactions are approximated by particle consideration. Lagrangian and Eulerian descriptions of motion are utilized to define the fluid flow motion in space and time.

According to Lagrangian description of flow motion in fluid dynamics, moving material points representing infinitesimally small fluid particles are kept tracked by the observer. Continuously capturing the position of the particles as it moves in fluid medium provides the flow path. This definition of motion can be considered as a recording of a human sitting in a boat and drifting down a river.

Eulerian description for flow motion is a way of looking at fluid particles from a fixed coordinate in the space through which the fluid particles flows [8, 9]. With the same analogy, the Eulerian description of motion can be thought in a way that an observer sitting on a bridge over a river and recording the water pass from that fixed location.

One of these methods for fluid flow description can be preferable to another depending on specific criteria such as tracking type, time history, type of geometry and boundary, and handling difficulty of the amount of deformation. In the Eulerian grid-based methods, the grids remain unchanged while the body deforms. In the Lagrangian description of deformation, we are interested in the motion of the particles without mesh.

2.2 Literature Review

2.2.1 Introduction

Over the years, computational methods have been proposed to solve differential equations applied engineering problems of solid mechanics and fluid dynamics. Fundamental idea of these techniques is to divide problem domain into a finite number of subdomains and solving a discrete form of the governing equations under prescribed boundary conditions.

Depending on the application area of the problem and its level of geometric and mathematical complexity, these techniques have been classified under various names such as finite difference methods(FDM), finite volume methods(FVM) and finite element methods(FEM).

The terminology associating the subdomain with imaginary regions varies depending on the method such that subdomain corresponds to an element, cell and mesh(grid) in FEM, FVM and FDM respectively. These subdomains are knitted in space with an imaginary web of nodal connectivity which is called mesh. The size of the mesh structure and type controls the solution wise error in numerical approximations.

In spite of the fact that the grid-based computational methods provide reliable solutions for many engineering applications, they may have some drawbacks when they are applied to the problems with a free surface, deformable boundary, moving interface, and extremely large deformation and crack propagation [62]. Furthermore, in grid-based methods, the complexity of the problem domain may cause difficulties in terms of meshing because of processing time [62].

Mesh generation is one of the fundamental requirements for the numerical solution of the mathematical models. In the Eulerian approach, fixed grid system over the problem domain is required and this causes additional effort to be able to determine inhomogeneous medium and distinguish free surfaces, deformable boundaries, and

moving interfaces. In many of the engineering problems, the main concern is to determine the material properties of the body. However, identifying these properties in a fixed domain becomes tough to keep track of the locations of the regional properties if the media is in a particle form [3, 25, 65]. In the grid-based Lagrangian methods, special additional treatments are needed to capture large deformation fields in solids and structures [61, 109] and this highly requires computational power.

Based on the complexity of the system and restrictions of grid-based methods such that the system has large deformations and inhomogeneities, moving material interfaces, deformable boundaries, and free surfaces, are challenging and treating these methods to obtain reliable results for such problems is expensive in terms of the computational time [105]. A more appropriate type of solution methods other than grid-based methods provide better treatments and can be considered more appropriate [2, 48].

2.2.2 Meshfree Methods

In the past, noteworthy research effort has been shown to the meshfree particle methods for more complex engineering problems with success [41, 59]. The key idea of using numerical methods is to give precise and reliable numerical results for provided boundary conditions [41, 59]. Wide range of scientific and engineering effort [41, 58, 59, 61, 80] related to the meshfree techniques already studied in the literature providing not only information related to improvement in the method but also the implementation of the method based on theoretical background.

One of the most recent studies in the literature is known as the gradient smoothing method(GSM) which applied to the gradient smoothing domains [60, 102]. The GSM technique can be coupled very well with an unstructured triangular grid and can be utilized successfully for versatile investigation [101].

2.2.3 Smoothed Particle Hydrodynamics

A modern, reliable and prominent meshfree method for computational applications on a continuum scale aiming to solve CFD problems based on Navier-Stokes equations is named as smoothed particle hydrodynamics or SPH. In the following subtitle, an overview of the method is introduced.

Smoothed particle hydrodynamics is viewed as the oldest meshless particle method known in history and applicable to continuum mechanics problems. Its invention and the first application were in the field of astrophysics where the scientists focused on making predictions regarding collective movement of particles in space similar to the liquid or gas media based on Newtonian physics [40, 70].

The SPH method defines the system in a way that it consists of a set of particles and each particle carrying the properties of the media in the system have interaction with others in the vicinity. The volume of the interaction vicinity is governed by a function named as kernel or smoothing function [37, 45, 63]. Since each particle possesses the vectorial and scalar properties of the medium such as local density, velocity, acceleration, all dependent quantities can be evaluated based on the interaction of the particles in the fluid media. For instance, fluid pressure is a function of the density of the fluid media and it can be calculated by means of equation state. It is also possible that the physical flow viscosity on the particle accelerations can be included in the calculations. In the SPH method, fluid surfaces and interfaces of two different fluids are also tracked by the particles that define the phases [62].

As an overview of the advantages of the SPH method over grid-based numerical approaches can be summarized by a couple of paragraphs as listed below [62].

- SPH is a particle strategy for Lagrangian nature. It can acquire the time history of the particles. The transport phenomenon of the systems in motion would thus be able to be captured in the time domain.
- The SPH method is an ideal computational technique to determine the motion characteristics of free surfaces and interacting liquids since the particles can be

deployed in specific locations inside the medium and can be marked, thus along the analysis, free surfaces and moving boundaries can be naturally tracked. The free surfaces, material interfaces, and moving limits can all be able to be tracked normally during the time spent reenactment, in any case, the complicity of the particle motion, which is hard to difficult for many Eulerian techniques.

- Fundamentally, SPH is a particle method and this method not to use a grid or mesh. As a result of this, it becomes an easy task to handle the problems with large deformations. The reason that the connection of the particles is inherently provided during the calculations. A couple of examples that SPH technique can be efficiently and appropriately applied in terms of its capability are explosion, underwater explosion, high-speed impact, and penetration problems.
- There can be found similarities between the meshless particle methods applied to the problems in different continuum scales and SPH technique. Molecular dynamics(MD) [1, 36] and dissipative particle dynamics(DPD) [44, 49] are the most known examples for those applications in the current literature . The reason for that application range of the SPH method can cover many engineering applications in a wide range.
- Compared to other numerical techniques used in the literature, the SPH method provides efficiency and easiness in terms of numerical implementations of in continuum mechanics not only two-dimensional but also three-dimensional problems.

The usage of the SPH method for numerical implementations was based on the calculations for probability theory and statistical mechanics applications. These formulations in which balance equations were not considered provided accurate results for the problems they were applied to. Moreover, it is challenging to implement the formulations of solid and fluid dynamics in terms of getting accurate and stable results. In time many other additions to the original formulations of the SPH method have been proposed to improve the performance of the method for different types of applications. Related to this, the conservation of momentum equation in the SPH method has been added in [39]. In addition to that, the implementation of the angular momentum in the SPH has been proposed by Hu and Adams for incompressible viscous flows [50]. Many scientific efforts associated with precision, strength, combination, and productivity of the SPH method can be found in the literature. For instance, in the field of mechanics, tensile stability of the solid materials was studied by Swegle et al. to figure out the

mechanical endurance of materials [94]. Morris et al. showed that the molecule irregularity issue that can prompt relatively poor precision in the SPH result [79]. In time, various adjustments or remedies have been attempted to reestablish the consistency and to enhance the exactness of the SPH outcomes. Monaghan proposed that better results can be obtained by applying formulations called symmetrization [73, 76, 77]. Johnson and his colleagues suggested a formulation for axis-symmetry normalization by which normal velocity strains became precisely reproducible for constant values of normal velocity strains [51, 52]. Formulations for normalization for density and divergence of stress tensor respectively have been derived by Randles and Libersky [89]. A corrective smoothed particle method (CSPM) by which the simulation precision both within the fluid domain and along its boundary regions get better has been offered by Chen et al [19, 20]. Following that, Liu et al offered an improved CSPM aiming to solve the problems including discontinuities. Such a method that deals with discontinuities occurring in the case of shock waves is known as discontinuous SPH (DSPH) [64]. A set of functions to provide an approximation for field variables has been offered by Liu et al. and the method that uses this set of equations was named as finite particle method (FPM) [66, 68]. A modified version of the SPH method for applications in solid mechanics has been introduced by Batra et al. It is considered that the method developed by Batra et al. has a similar idea to FPM and it is introduced as modified SPH (MSPH) [11]. When FPM compared to the CSPM method, it can be considered as the upgraded version in terms of fulfillment in particle compatibility. Also, Fang et al. conducted studies for improving numerical analysis for free-surface flow problems [33] and then they proposed a method called regularized Lagrangian finite point method for simulation of incompressible viscous flows [34, 35]. For the problems known as zero energy in the literature, a technique which is named stress point method has been offered to enhance tensile stability [30, 31, 88, 97]. There are many other remarkable studies to provide improvements in the SPH method, some of those are moving least particle hydrodynamics (MLSPH) [27, 28], correcting kernel integration [17], the reproducing kernel particle method (RKPM) [21, 69], an approach for correction of stable material points [13, 87] and other approaches for restoring the consistency [45, 66, 104]. In the literature, Belytschko et al. provided many studies regarding stability and convergence of meshfree particle methods and it has been shown that it is possible to apply some of those numerical methods and type of analyses to SPH method as well [12–14].

2.2.4 Overview of Water Entry Problem

A high level of importance has been attributed to the water entry problem of a wedge geometry with a significant amount of study in the literature since the time of von Karman who is considered as one of the pioneering scientists with his valuable contributions in the field of fluid dynamics. The significance of the water entry problem for the wedge-shaped geometries comes especially from the aim of the determination of slamming forces in ship hydrodynamics applications. Related to this, it is the fact that outcomes of numerical analyzes can provide information regarding local forces distributed over the load-carrying elements of the ship structure and all this ensure input data associated with the structural and operational design of the ships [81].

At the instant the wedge geometry engages in the water surface, the force transferred into liquid media can be computed through the balance of momentum. During the transformation of momentum it can be assumed that the wedge geometry is integrated into liquid mass, which is known as the added mass method in the literature.

Beyond the idea of determination of the impact loadings on a wedge geometry, investigation of jet formation and its scattering around the entry region was studied by Wagner [100]. In this study predicted pick pressure value by Wagner was associated deadrise angle.

Garabedian proposed to express the physical properties of a fluid in terms of dimensionless parameters, leading to an understanding of the impact phenomenon in a straightforward fashion. Garabedian's proposal was further developed upon the study by the Wagner who had been utilized from conformal mapping [38].

Following Garabedian's work in 1957, Borg's contribution provided an iterative solution scheme for Laplace's partial differential equations for the water entry problem of a wedge unsymmetrically engaging in still water surface. The outcomes of Borg's study showed good agreement with experimental results of the wedges entering into the water with 45° and 80° deadrise fronts [18].

Dobrovolskaya was the first name who firstly offered an analytical solution for wedge entry problem in two-dimensional domain [29]. Despite the fact that significant contributions to numerical and analytical solutions regarding water entry problem, none of those could achieve capturing pile-up, separation of water and formation of spray around the wedge body.

For simple vee-shaped wedges with various deadrise angles between 10° to 50° high-speed camera system which were capable of recording 1500 frame per second had been utilized to capture the motion for vertically dropped bodies [16]. The studies in the context of numerical investigation of the acceleration for the vee-shaped wedge body showed consistency with the outcomes of Wagner's experimental study in 1932.

Experimental investigations revealed that during the vertical motion of the wedge geometry towards the quiescence water air squeezed underneath the wedge was compressed in such a way that the peak pressures and accelerations were affected and resulted in fewer values than they were supposed to be calculated theoretically. Then the context of the experimental studies was conducted to include the cases of wedge geometries with deadrise angles less than 10° . Following those studies, a flat panel was subjected to free fall by Chuang under the effect of gravitational forces so that due to the air cushion effect less liquid pressure was recorded than the pressure von Karman expected in his early study [23, 24]. Under the effect of compressed air beneath the wedge body, Chuang further extended his investigations to capture liquid pressure and wedge accelerations for varying deadrise angles ranging from 1° to 15° .

The earlier studies indicated that the CFD models could not provide accurate results in terms of fluid pressure for the entry problem of wedges having deadrise angles less than 15° . Furthermore, for solid wedges with deadrise angles less than 15° single-phase liquid models were less capable in terms of modeling than the models including two phases in their solution algorithm and more reliable solutions can be obtained when air medium is included in the problem domain.

In the following years, Chuang also continued his studies with geometries in cone-shaped and the correction for the air compressed underneath the cone geometry was not considered in the solution [22]. Chuang showed that approximating a cone to a flat

plate by using conformal transformation provides similar solutions in terms of pressure distribution Wagner provided [100].

In addition to the added mass approaches until his time, Payne [86] revealed that based on experimental investigations performed by Bisplinghoff and Doherty [16] sophisticated versions of added mass approaches compared to the results of von Karman [99] and Wagner [100] provided less reliable outcomes. Insertion of a force component into the numerical model provided more consistency with the experimental study by Bisplinghoff and Doherty [16]. Even though the remarkable improvement was obtained in terms of results based on the proposed numerical model, predictions over the form of water separation and jet profile could not be obtained through the model provided.

Greenhow [42], Vinje and Brevig [98] implemented Cauchy's theorem in two-dimensional water entry problem to be able to obtain a solution for the integral of an analytical function circulating a close region. The analytical function integrated with Cauchy's theorem utilized in the proposed model, carrying both complex velocity potential and streamline function characteristics, resulted in consistently with experimental data obtained at 45° , 60° and 81° deadrise angles.

Instead of using added mass method Wagner [100] used in his model, a finite difference method over an ordinary grid base was implemented by Arai and Tasaki [7] for the purpose of identifying generated loads over a wedge subjected to free falling.

An advantage of using Arai and Tasaki [7] method in comparison to Wagner's proposed technique [100] is that formulations can be easily implemented for a body in specific geometry like bow-shaped. Even though FDM showed its capability to capture loads and pressure distributed over the wedge geometry, large deformations and fracture could not be resolved since the technique is based on grid-based methods.

A study in relation to the solution for deformation of a free surface in the transient characteristic is performed based on a fractional volume of the fluid method by Arai et al [5]. The technique is applied on geometries in various shapes such as a circular cylinder, a 30° deadrise wedge, a 45° deadrise wedge and a ship bow section. Comparison of the fractional volume of the fluid method to Wagner [100] showed that Arai et al.'s proposed

method provides a good correlation for all excluding bow section shaped while added mass method does not provide a solution for the motion of the bow-shaped body. The VOF technique proposed by Arai et al. [7] is implemented for the purpose of minimizing slamming forces on the load-carrying elements of the ship structure [6], revealing that impact loads were reduced to half of a cylinder in case of using parabolic members. Following the study by Arai et al. [6], the geometry of the body engaging in calm water is decided to be in the form of U, V and large bow sections of a ship.

Wedge entry problem is found to be important for the determination of the limits in terms of structural endurance of offshore bodies since solutions out of analyzes provide useful input to structural architecture. In open sea conditions, ships and other offshore structures are imposed to harsh loadings when swashing occurs over the free water surface. Loads that occur during the slamming between the water and sea structure can produce high stresses through the load-carrying elements of the body. Thus, determination of the slamming pressures over the vehicle body is important since it provides criteria for structural design. Because of the estimation of these local loadings which can occur suddenly in the open sea conditions and their non-linear characteristic it can be challenging to perceive the catastrophic effects on the structure. Studies regarding water entry problem can be found in the current literature and validation of the CFD solutions are provided through commercial software. For instance, Shen et al. performed simulations in two and three-dimensions to generate estimated pressure values for different ships sections which were allowed to be dropped from varying heights [108].

A technique which is called immersed boundary method was offered by Zhang et al. for the investigation of flow motion of free surfaces when solid objects having arbitrary shape are allowed to engage in fluid media, [106]. Implementation of the method for capturing free surface motion has been coupled with their improved immersed boundary method. In this way, the solver using Navier-Stokes equations and coupled with advanced method enabled the solid-fluid interaction for arbitrary objects to be numerically analyzed. Zhang et al. offered to use an algorithm that applies the forces to the particles locating in the immediate vicinity of the solid boundaries. Thus, precise solutions with accuracy have been obtained. Besides the interaction of objects having arbitrary bodies with fluid phase, the same numerical model has been applied for the analysis of vertical forces and pressure distribution due to slamming motion of

a wedge. As a result, the obtained results out of numerical study have been compared with experimental outcomes as well.

One another numerical study based on the finite volume method on the investigation of water entry of objects having wedge and circular geometries is presented by Kleefsman by et. al., where formulas of Navier-Stokes have been used as governing equations to define the flow motion of incompressible viscous media [53]. For the method utilized in this study, stability and precision are strictly associated with the boundary conditions at the free surfaces which are moved by means of the Volume-of-Fluid method. The wedge geometry with varying dead-rise angles and circular shaped objects are separately subjected to drop with free-falling into calm water with a determined velocity. The outcomes of the experimental study, [43] performed by Greenhow et. al., which presents the photographs of the side splashing of water under the effect of wedge penetrating into the calm water surface has been correlated with simulation results and theoretically obtained slamming coefficients are compared.

A study aiming to build a numerical model for simulation of free-surface flow around a solid object floating inside liquid media is presented by Liu et al. [67]. Thanks to its meshfree and Lagrangian based approach, the SPH method is inherently capable of capturing large scale deformations and objects following arbitrary paths prescribed by governing equations based on Navier-Stokes formulations. Because of the nature of the technique, it does not require any further treatment to embed into the scheme of the numerical solver to capture the free moving boundary or object in the simulations. It is also possible to consider all degrees of freedoms associated with the dynamic movement of the solid particles resulting in simulation of the rigid objects in motion and which may interact with surrounding media as well. In this study, they applied a model for turbulence flow called Reynolds-averaged Navier–Stokes and beside adjustments on kernel-related functions and offered developed solid boundary conditions. The problems and their numerical implementations that they covered in this study include simulation of a cylindrical shaped object during its exit out of the water, the arbitrary motion of an elliptical-shaped geometry inside liquid media and immersion of a cylinder into calm water. The results obtained in the study provide a good consistency with the results of distinct research in the literature.

Free surface flow case at the boundary of a wedge geometry exposed to interaction

with fluid media is numerically simulated by means of smoothed particle hydrodynamics method, [81], where particle sampling scheme is applied and the method is configured to estimate fluid pressure distribution over the wedge boundary. The formulations aiming to monitor the dynamic effects of freely moving boundaries are integrated into the SPH scheme. Oger et. al. offered a set of equations formulating a scheme where resolution changes spatially with varying smoothing length. Verification of the SPH scheme configured with new integrations is provided through the entry of the wedge geometry for two different cases. Pressure distributions along the wedge boundary and pressure field on the liquid domain based on analytical and experimental results in the literature have been compared with the outcomes of the numerical analysis. In addition to that, a discussion regarding the correlation of the results is provided for the penetration of the wedge geometry to calm water.

A numerical study presented by Tofighi et. al where a combination of rigidity and viscous penalty constraints are included in the SPH method, which simulates the motion of rigid bodies inside fluids in Newtonian characteristic [96]. Different types of movement characteristics of the solid objects such as linear, rotational and their combination to test the robustness of the proposed coupling of the SPH method with the rigidity and viscous penalty algorithms have been investigated. One of the test cases presented in the study covers free-falling off a pair of circular discs following each other during their sedimentation through a calm liquid medium. The study reveals that the proposed SPH scheme is capable of simulating precipitation of circular and elliptic shaped bodies at different Reynolds numbers in an accurate manner.

An experimental study revealing pressure distribution along the angled surfaces of a wedge which falls freely into quiescent water surface [103]. The pressure data induced by the impact on the water surface is collected by the transducers placed along the angled surface of the wedge. In the water entry problem, the pressure caused by the water impact on the wedge side can be associated with a set of parameters such as drop height, deadrise angle and the mass of the wedge. In the study, the results of the experiment conducted to investigate pressure distribution during the water entry of a wedge have been compared to outcomes of numerical models in the literature.

3. SMOOTHED PARTICLE HYDRODYNAMICS

The following is a detailed introduction to the meshless Lagrangian particle method Smoothed Particle Hydrodynamics (SPH) to solve PDEs widely applied to different areas in engineering and science. In this chapter, the basic idea of the SPH method and its fundamental formulations are introduced.

3.1 Integral Representation of a Function in SPH Method

Fundamentally, the SPH method is based on interpolation. From the SPH point of view, any field function is obtained by averaging the functional values of particles which are randomly distributed over a defined region through a weight function. The weight function, $W(r_{ij}, h)$ is defined as a function which becomes equivalent to the Dirac Delta function, δ , as the interpolation or smoothing length, h , approaches to 0. Mathematically, the following statement can be written for any continues function, $f(r_i)$, which can be scalar, vector, or tensor-valued function.

$$f(\vec{r}_i) = \int_{\Omega} f(\vec{r}_j) \delta(\vec{r}_j - \vec{r}_i) d^3 \vec{r}_{ij} \quad (3.1)$$

$$\int_{\Omega} \delta(\vec{r}_j - \vec{r}_i) d^3 \vec{r}_{ij} = \begin{cases} 1, & \vec{r}_j = \vec{r}_i \\ 0, & \vec{r}_j \neq \vec{r}_i \end{cases} \quad (3.2)$$

In this equation $r_{ij} = r_j - r_i$ is the distance vector between two particles while the indices i and j represents the particles' identities. More specifically, the i index indicates the particle interested in while the index j denotes the others which interact with the particle i .

If the Dirac delta function given in Equation (3.2) is replaced by a smoothing kernel function, given by $W(r_{ij}, h)$, the integral estimate or the kernel approximation to an arbitrary function f_i can be introduced as

$$f(\vec{r}_i) \cong \langle f(\vec{r}_i) \rangle \equiv \int_{\Omega} f(\vec{r}_j) W(r_{ij}, h) d^3 \vec{r}_{ij} \quad (3.3)$$

where the bracket sign, $\langle \rangle$ states SPH approach while $d^3 \vec{r}_{ij}$ represents the infinitesimal volume element within the interaction region of the interested particle. Meanwhile, the Ω sign indicates the volume of this interaction region. The field function, f_i may stand for hydrodynamic quantity such as velocity, density, pressure or viscosity.

In this integral approximation, accuracy of the error is $O(h^2)$, providing 2nd degree convergence, [95]. The error term is obtained by applying Taylor series expansion on $f(\vec{r}_j)$ around r . Using Equation (3.3) leads to

$$\langle f(\vec{r}_i) \rangle \equiv \int_{\Omega} W(r_{ij}, h) \left\{ f(\vec{r}_i) - \frac{\vec{r}_i - \vec{r}_j}{h} f'(\vec{r}_i) + \frac{(\vec{r}_i - \vec{r}_j)^2}{h^2 2!} f''(\vec{r}_i) + \dots \right\} d^3 \vec{r}_{ij} \quad (3.4)$$

The condition that the weighting function $W(r_{ij}, h)$ to be positive and even, the odd terms in Equation (3.4) should equal to zero. The dominant error term is the 2nd order expression. In order to obtain an error term of this order, the weight function should be created and the second-moment value given in the Equation 3.5 should be equal to zero.

$$\int_{\Omega} r_{ij}^2 W(r_{ij}, h) d^3 \vec{r}_{ij} = 0 \quad (3.5)$$

In order to calculate the derivative of a function in SPH method, using the approach defined in Equation (3.3), if the derivative of this function is written instead of $A(\vec{r}_i)$, we obtain

$$\frac{\partial f(\vec{r}_i)}{\partial x_i^k} \cong \langle \frac{\partial f(\vec{r}_i)}{\partial x_i^k} \rangle \equiv \int_{\Omega} \frac{\partial f(\vec{r}_j)}{\partial x_i^k} W(r_{ij}, h) d^3 \vec{r}_{ij} \quad (3.6)$$

In this equation, the upper index, k , indicates the components of the position vector. If the integration of the weight function is equal to zero and the interpolation length (h) is taken as constant, taking advantage of $\partial W(r_{ij}, h)/\partial x_i^k = -\partial W(r_{ij}, h)/\partial x_j^k$, the equation is transformed into the Equation 3.6 and if partial integration is applied and the Equation 3.6 becomes the following.

$$\frac{\partial f(\vec{r}_i)}{\partial x_i^k} \cong \langle \frac{\partial f(\vec{r}_i)}{\partial x_i^k} \rangle \equiv \int_{\Omega} f(\vec{r}_j) \frac{\partial W(r_{ij}, h)}{\partial x_i^k} d^3 \vec{r}_{ij} \quad (3.7)$$

The same approach is used for taking higher-order derivatives and only the desired function of weight function is obtained and the process is completed.

3.2 Particle Approximation

In the SPH method, integral equations of continuous functions are discretized by using particle approximation. In the Equation (3.3), ΔV_j is written instead of $d^3 r_{ij}$ representing the infinite small volume in the region in which the weight function is defined, and the mass of this particle is shown as follows.

$$m_j = \Delta V_j \cdot \rho_j \quad (3.8)$$

In the Equation 3.8, ρ_j is the density of the particle ($j = 1, 2, \dots, N$). N represents the number of particles existing in the interaction region of the particle j . In this manner, the particle approach is stated as below.

$$f(\vec{r}_i) \cong \int_{\Omega} f(\vec{r}_j) W(r_{ij}, h) d^3 \vec{r}_{ij} \cong \sum_{j=1}^N f(\vec{r}_j) W(r_{ij}, h) \Delta V_j \quad (3.9)$$

In the Equation (3.9), if the expression in the Equation (3.8) is replaced by ΔV_j , the function value of any i particle in the SPH terminology is approximately written as follows.

$$\langle f(\vec{r}_i) \rangle = \sum_{j=1}^N f(\vec{r}_j) \frac{m_j}{\rho_j} W(r_{ij}, h) \quad (3.10)$$

With the same approach, we can write a derivative of a function as follows.

$$\frac{\partial f(\vec{r}_i)}{\partial x_i^k} \equiv \langle \frac{\partial f(\vec{r}_i)}{\partial x_i^k} \rangle \cong \sum_{j=1}^N f(\vec{r}_j) \frac{m_j}{\rho_j} \frac{\partial W(r_{ij}, h)}{\partial x_i^k} \quad (3.11)$$

3.3 Application of Particle Approximation to Governing Equations

At this part of the study, SPH method is applied to the governing equations of fluid motion and discrete form of the formulations will be introduced. Known as the continuity equation is expressed by

$$\frac{d\rho}{dt} + \rho \nabla \cdot \vec{u} = 0 \quad (3.12)$$

where \vec{u} is particles velocity vector, $d/dt = \partial/\partial t + \vec{u} \cdot \nabla$ represents the material time derivative and ρ is the density of particles.

In the SPH method, there are two approximation ways of density function changing, [74]. The first approach is called "summation density" and it is obtained by replacing $f(\vec{r}_i)$ term with density in Equation (3.10). And, the summation density is expressed as follows.

$$\langle \rho_i \rangle = \sum_{j=1}^N m_j W(r_{ij}, h) \quad (3.13)$$

According to this equation, the density of a particle at point i is calculated by taking a weighted average of all the particles adjacent to it.

Particle approximation can be also provided by one another method which computes the change in density. Approximation scheme is implemented through Equation (3.12). Combination of the SPH method with the expression given by $\nabla(\rho \mathbf{u}) = \rho \cdot \nabla \mathbf{u} + \mathbf{u} \cdot \nabla \rho$ provides the change in density. For any given particle i the density with continuity approach is given by

$$\left\langle \frac{d\rho_i}{dt} \right\rangle = \rho_i \sum_{j=1}^N \frac{m_j}{\rho_j} (\vec{u}_i - \vec{u}_j) \cdot \nabla_i W_{ij} \quad (3.14)$$

Both approaches have their own advantages and disadvantages. Since the density is calculated by the integration of the masses of all particles within a defined region, while the mass is fully conserved, in the continuous density approach, mass conservation may not be fully realized, [62]. Against this, in the total density approach, there may be an effect called the edge effect in the areas near the boundary of the fluid, causing the density to disappear completely and therefore to very large displacement and velocity values. Edge effect, the intensity of particles in these regions can not be accurately calculated due to the decrease of their neighborliness in areas near the borders where particles can interact. However, the edge effect event can be prevented by using virtual boundary elements or some other methods. In addition, since the total density approach calculates the density of all particles and the weight function values in order to calculate other area variables at each time step, the computer solution time takes longer than the

continuous density approach, [62]. In the solution of the problems that this study dealt with, a continuous density approach was used to avoid boundary impact and to reduce calculation costs. However, the density values obtained as a result of this approach have been corrected with a correction algorithm which will be explained in detail.

Another important equation representing the movement is the momentum conservation equations. These equations can be written as including viscous effects (Navier-Stokes) or without inclusion (Euler). In general form, momentum conservation equations including viscous effects are expressed as follows:

$$\frac{d\bar{\mathbf{u}}_i}{dt} = \frac{1}{\rho} \frac{\partial \mathbf{T}_{ij}}{\partial x_j^k} + \bar{\mathbf{F}}_i \quad (3.15)$$

$\bar{\mathbf{F}}_i$ indicates body force which applied to unit mass and \mathbf{T}_{ij} is stress tensor as given in Equation (3.16),

$$\mathbf{T}_{ij} = -p\delta_{ij} + \sigma_{ij} \quad (3.16)$$

where p , δ_{ij} , μ , and σ_{ij} are pressure, unit tensor, viscosity coefficient, and viscous tensile tensor respectively.

$$\sigma_{ij} = \mu \left\{ \left(\frac{\partial u_i}{\partial x_j} - \frac{\partial u_j}{\partial x_i} \right) - (\nabla \cdot \mathbf{u}) \delta_{ij} \right\} \quad (3.17)$$

In the standard symmetric SPH method, the expression on the right side of the conservation equation, extraction can be carried out using the feature given below with the vector representation, [93]:

$$\frac{1}{\rho} \nabla \cdot \mathbf{T} = \nabla \cdot \left(\frac{\mathbf{T}}{\rho} \right) + \left(\frac{\mathbf{T}}{\rho^2} \right) \cdot \nabla \rho \quad (3.18)$$

By using SPH approximation, the two terms to the right-hand side of Equation (3.18) can be written as follows:

$$\nabla_i \cdot \left(\frac{\mathbf{T}_i}{\rho_i} \right) = \sum_{j=1}^N m_j \left(\frac{\mathbf{T}_i}{\rho_i^2} \right) \cdot \nabla_i W_{ij} \quad (3.19)$$

$$\left(\frac{\mathbf{T}_i}{\rho_i^2} \right) \cdot \nabla \rho_i = \frac{\mathbf{T}_i}{\rho_i} \cdot \sum_{j=1}^N m_j \nabla_i W_{ij} \quad (3.20)$$

Finally, when these terms in Equation (3.15) are replaced on the right side of the conservation equation. As a result, the corresponding expression of the Navier-Stokes equations in the SPH method is obtained:

$$\frac{D\vec{u}_i}{Dt} = \sum_{j=1}^N m_j \left(\frac{\mathbf{T}_i}{\rho_i^2} + \frac{\mathbf{T}_j}{\rho_j^2} \right) \cdot \nabla_i W_{ij} \quad (3.21)$$

When the effects of viscous were neglected, the Euler's equation of motion may be discretized by the SPH method to provide the following relation:

$$\frac{D\vec{u}_i}{Dt} = - \sum_{j=1}^N m_j \left(\frac{p_i}{\rho_i^2} + \frac{p_j}{\rho_j^2} \right) \cdot \nabla_i W_{ij} \quad (3.22)$$

Another expression given in the literature of Euler equations is given as follows [62]:

$$\frac{D\vec{u}_i}{Dt} = - \sum_{j=1}^N m_j \left(\frac{p_i + p_j}{\rho_i \rho_j} \right) \cdot \nabla_i W_{ij} \quad (3.23)$$

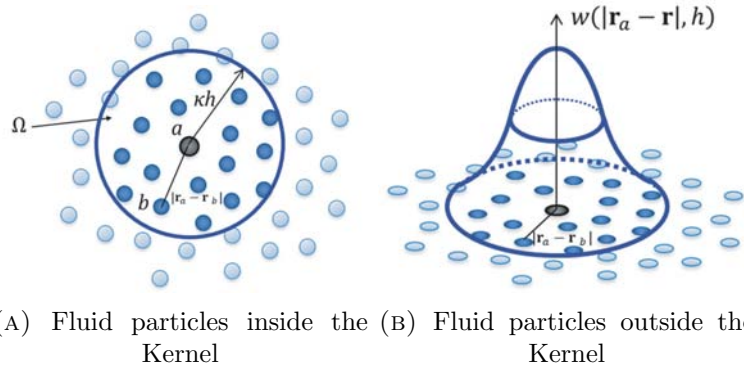


FIGURE 3.1: Visual representation of a Kernel function,[32]

As seen, the most important feature of both momentum equations is that the equation is symmetric for i and j particles. In other words, the i and j particles in the system the forces they exert on each other are equal in magnitude and opposite in direction. This due to the feature, momentum protection can be fully achieved.

3.4 Weight (Kernel) Functions in SPH Methods

Kernel in the SPH method - as used previously in Equation (3.3) - provides accuracy for the statement of the function and affects the performance for the computation., [56], [62]. A kernel-function approach defines the area of each particle as seen in Figure (3.1) while the neighboring particles appearing in blue color around grey color are illustrated. Each particle is assumed to interact with others in a spherical volume determined with a radius called smoothing length. Depending on the distance between a couple of particles, the contribution of physical properties on the particle of interest varies. Kernel functions have some major requirements which are summarized as follows, [92], [63].

- **Normalization condition:** Normalization upon the support domain is applied to the smoothing function.
- **Compact support:** Compact support condition is implemented to the kernel as defined below.

$$W(r - r', h) = 0 \quad \text{if } |x - x'| > \kappa h \quad (3.24)$$

κ is a constant which determines the spread of the specified smoothing function and the κh defines the radius of this domain.

- **Positivity:** Kernel function is always defined as equal to or greater than zero within its support domain and the positivity condition is provided as follows.

$$W(r - r', h) \geq 0 \quad (3.25)$$

- **Decay:** Reverse proportionality is defined in a way that value of the smoothing function decreases while the distance of the interacting particles increases.
- **Delta function property:** Dirac delta function provides a characteristic property for the kernel function while smoothing length goes to zero. Mathematically, this condition is expressed as follows.

$$\lim_{h \rightarrow 0} W(r - r', h) = \delta(r - r') \quad (3.26)$$

- **Symmetric property:** The kernel function has to be spherically symmetric even function.
- **Smoothness:** The smoothing function should be sufficiently smooth.

The function satisfying the conditions given above can be used as a weighting function in the SPH method. These properties provide Better estimations of the function and its spatial derivatives are provided by these properties. In this manner, a sufficiently continuous weighting function needs to be chosen in order to obtain good results.

In the SPH method, selection of the weight function, $W(r_{ij}, h)$, and determination of smoothing length of interacting particles are important issues in terms of convergence of the results. Although there are numerous examples of weight function in the literature, [62], some examples that range from the simple Gaussian kernel to complex 3rd and 5th order spline functions will be given below. For instance, the Gaussian kernel given by the equation, was referred to as the best approximation in terms of numerical stability and convergence for three-dimensional problems, [77].

$$W(R, h) = \frac{1}{\pi^{\frac{3}{2}} h} \left(\frac{5}{2h^2} \right) \exp(-R^2) \quad (3.27)$$

where relative distance between coordinates of the particles at reference (x) and deformed states (x') is given by R and defined as $R = r/h = |x - x'|/h$. Theoretically, Gaussian kernel is not really compact because when R approaches to infinity, it goes to zero. However, if the function is close to zero very fast in numerically, this region can be easily identified. The only disadvantage of this function is that it takes a long time to calculate higher-order derivatives of the function [45]. In Figure 3.2, Gaussian weight function and its derivative is given.

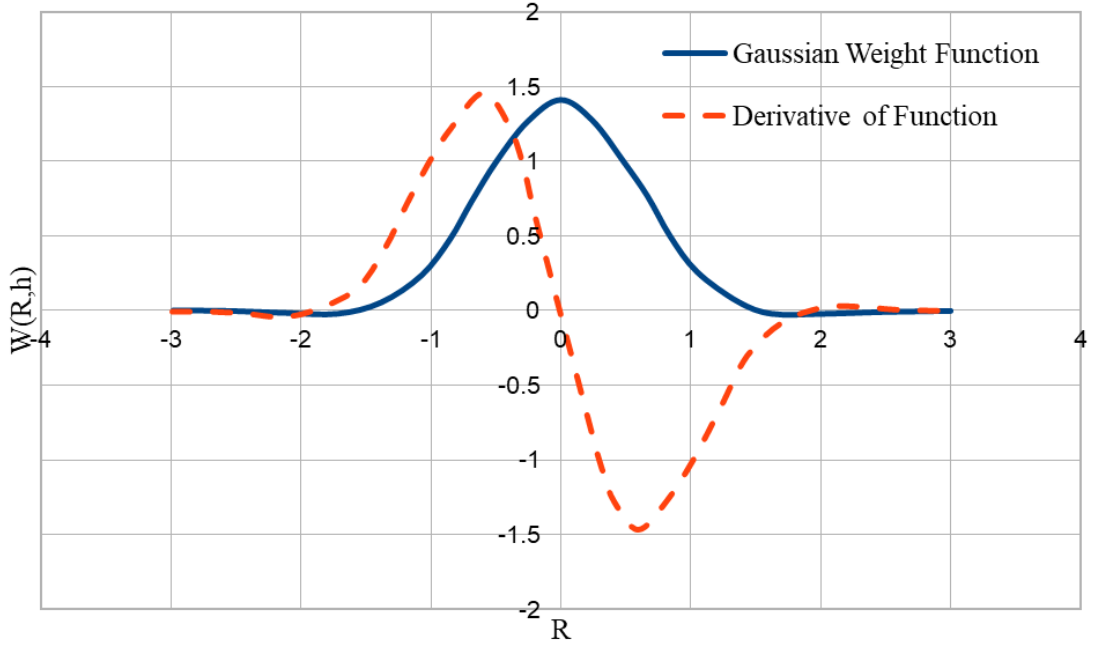


FIGURE 3.2: The function of Gaussian kernel and its derivative

An example of another weight function is the example of the cubic-spline weight functions created in [78] where the batching curves are used. The function for the cubic kernel is given in Equation 3.28 while the graph of its derivative is presented in Figure 3.3.

$$W(R, h) = \alpha_d \begin{cases} \frac{3}{2} - R^2 + \frac{1}{2}R^3, & 0 \leq R < 1 \\ \frac{1}{6}(2 - R)^3, & 1 \leq R < 2 \\ 0, & R \geq 2 \end{cases} \quad (3.28)$$

As can be seen, this function is a 3rd degree function and it is designed as a piecewise. Lastly, it is also used in [85], and the quintic Kernel is given by Equation 3.29 and used in this study, the graph of the function and its derivative is given in Figure 3.3.

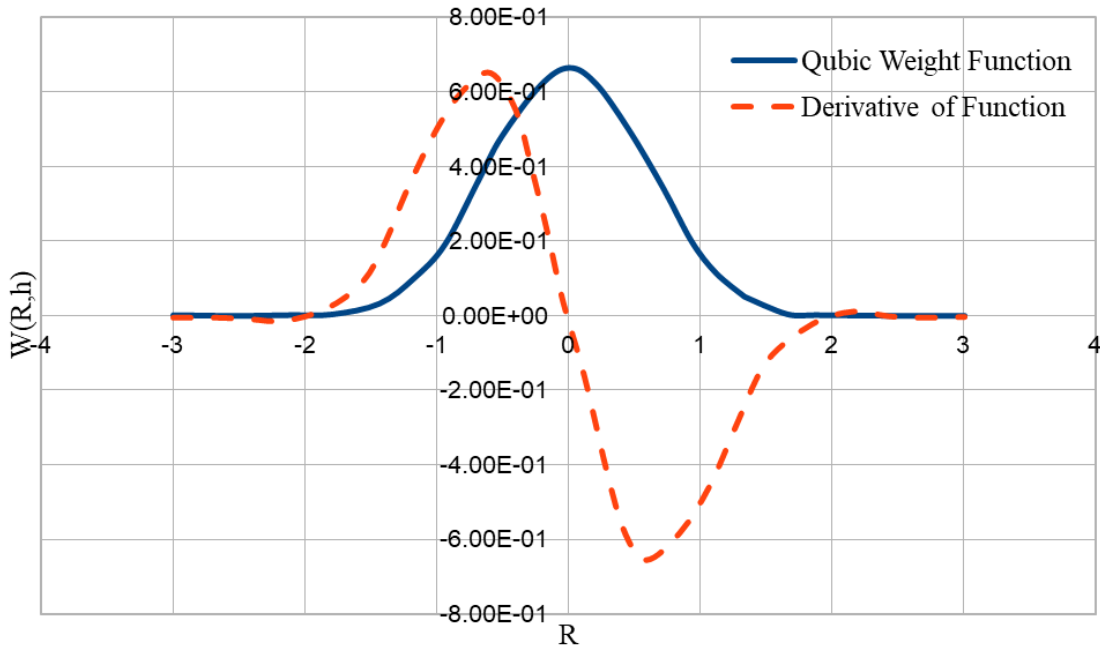


FIGURE 3.3: The function of cubic kernel and its derivative

Despite its computationally expensive characteristic compared to others, one of the reasons that the following quintic weighting function in this recent study is used is that it gives more reliable and precise results. The one another reason why the following weighting function is utilized is that it has high numerical stability.

$$W(R, h) = \alpha_d \begin{cases} (3 - R)^5 - 6(2 - R)^5 + 15(1 - R)^5, & 0 \leq R < 1 \\ (3 - R)^5 - 6(2 - R)^5, & 1 \leq R < 2 \\ (3 - R)^5, & 2 \leq R < 3 \\ 0, & R \geq 3 \end{cases} \quad (3.29)$$

where $R = |r_{ij}|/h = |r_j - r_i|/h = |x - x'|/h$, a_d is a coefficient which alters depending on size of the problem under consideration. This coefficient is taken as $7/(478\pi h^2)$ for two dimensional problems.

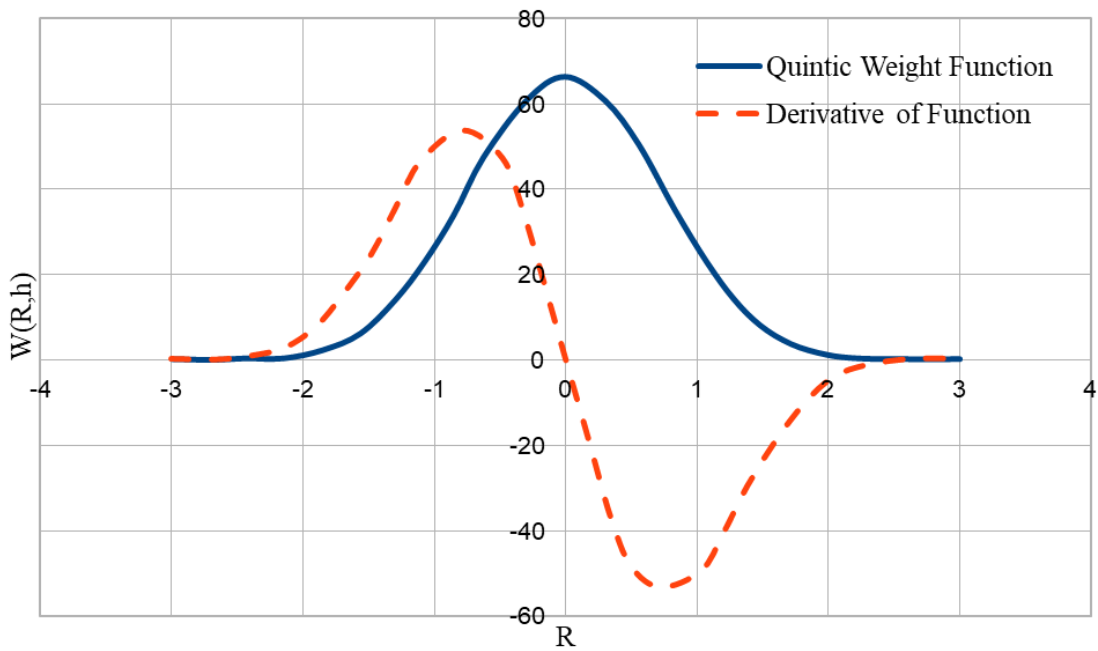


FIGURE 3.4: The function of cubic kernel and its derivative

3.5 Mathematical Modelling

3.5.1 Governing Equations

As previously introduced, continuity and Navier Stokes equations constitute a cornerstone for numerical simulations of flow motion. This set of equations that govern

the flow motion will be utilized in the mathematical modeling of the fluid problem under consideration. In the free-surface fluid flow problems, the continuity equation in which the statement of conservation of mass is stated as follows.

$$\frac{d\rho}{dt} + \rho \nabla \cdot \vec{u} = 0 \quad (3.30)$$

Furthermore, the Navier-Stokes equation stating the balance of linear momentum of a liquid particle is expressed by

$$\frac{d\vec{u}}{dt} = -\frac{1}{\rho} \nabla p + \nu \nabla^2 \vec{u} + \vec{g} \quad (3.31)$$

This set of equations and the Navier-Stokes statement for fluid motion will be explicitly presented for the mathematical formulation of fluid motion in the following sections.

Displacement of the fluid particles is provided by the following equation.

$$\frac{d\vec{r}}{dt} = \vec{u} \quad (3.32)$$

where \vec{u} , p , ν , ρ and \vec{r} and \vec{g} terms represent velocity vector, pressure, kinematic viscosity, density, positions of the particles and gravitational acceleration respectively. The pressure field in the SPH method is calculated by means of two distinct approaches that are named as fully [26] and weakly compressible [74] approaches.

The pressure value in the Navier-Stokes formulation of motion given by Equation 3.31 has been proposed to be calculated by means of the following state equation, [10].

$$p = \frac{\rho_0 c_0^2}{\gamma} \left[\left(\frac{\rho}{\rho_0} \right)^\gamma - 1 \right] \quad (3.33)$$

In this equation, c_0 , ρ_0 refers to reference values of speed of sound[m/s] and water density respectively while gamma is a coefficient whose value is assigned to 7. Also,

the reference value of water density is taken as 1000 [kg/m³]. The reference value of the speed of sound should be chosen as much as big that keeps the change in particles' densities with respect to reference density value in the range of $\pm 1\%$. This condition can only be satisfied when the Mach number is smaller than 0.1. In other words, the reference speed of sound should be assigned to a value which is 10 times bigger than the fastest particle speed [75]. In this recent study since many wave system simulations in different characteristics have been performed, c_0 reference speed of sound is determined to be 40 times of the generated wave speed by the system.

3.5.2 SPH Approximation and Discretization of Momentum Equations

The equations of motion can be separated and expressed in a discrete form under the fundamental principles of the SPH method as follows.

$$\frac{d\rho_i}{dt} = \rho_i \sum_{j=1}^N (\vec{u}_i - \vec{u}_j) \cdot \nabla_i W_{ij} V_j \quad (3.34)$$

$$\rho_i \frac{d\vec{u}_i}{dt} = - \sum_{j=1}^N \left(\frac{p_i}{\rho_i^2} + \frac{p_j}{\rho_j^2} \right) \nabla_i W_{ij} V_j + K\nu \sum_{j=1}^N \Pi_{ij} \nabla_i W_{ij} V_j + \rho_i \vec{g} \quad (3.35)$$

The N term in the equations given above indicates the number of particles within the interaction region of the interested particle. ∇_i is the gradient operator taken with respect to the position of particle i , $K = 2(n + 2)$ where n is the dimension of the problem domain. V_j indicates the volume of particles which is calculated by the formula $V_j = \sum_{i=1}^N 1/W_{ij}$ and Π_{ij} is the viscosity term which is defined as [4],

$$\Pi_{ij} = \frac{(\vec{u}_j - \vec{u}_i) \cdot (\vec{r}_j - \vec{r}_i)}{\|\vec{r}_j - \vec{r}_i\|^2} \quad (3.36)$$

The value of the kinematic viscosity, ν , is taken as 10^{-6} [m²/s] for water.

3.6 Corrective Numerical Algorithms

In this subsection, it will be briefly mentioned the correction terms added to the algorithm to be able to enhance stability, precision, and correctness of the numerical solution schematic of SPH. The correction terms that will be introduced in this subsection are going to be derivative, density, free water surface, and particle transnational corrections.

3.6.1 Gradient Correction of Weight Function

Although in the SPH method, a function defined in the problem region can be represented with second-order $O(h^2)$ convergence by means of an approximation based on interpolation technique, some corrections are needed to be able to reach the same convergence level in the derivative of the same function. [67]. In this study, the derivative of the weighting function given by Equation 3.4 is corrected by multiplying it with reversible $L(r_i)$ matrix which is obtained by means of Taylor series of expansion:

$$\nabla^c W_{ij} = L(\mathbf{r}_i) \nabla_i W_{ij} \quad (3.37)$$

$$L(\mathbf{r}_i) = \left[\sum_j \begin{pmatrix} x_{ji} \frac{\partial W_{ij}}{\partial x_j} & y_{ji} \frac{\partial W_{ij}}{\partial x_j} \\ x_{ji} \frac{\partial W_{ij}}{\partial y_i} & y_{ji} \frac{\partial W_{ij}}{\partial y_i} \end{pmatrix} V_j \right]^{-1} \quad (3.38)$$

Discrete form of the equations of motion expressed in the differential expressions of weighting function given by Equations 3.34 and 3.35 are used in derivatives of corrected weighting function constructed by Equation 3.37. In Equation 3.38, V_j stating the particle volume is calculated by the expression $V_j = \sum_{j=1}^N = 1/W_{ij}$.

3.6.2 Density Correction

In the weakly compressible SPH approach, the pressure values are calculated by means of the densities which are coupled with the equation of state given by Equation 3.33. This necessitates the density values to be calculated with high precision. Otherwise, solutions may not be able to obtain because of high fluctuations in the pressure field and noise leading to numerical instabilities [83]. (Density correction algorithms are used to be able to resolve this difficulty) This difficulty can be resolved by means of density correction algorithms frequently used in the SPH literature ([4], [72]). The density correction algorithm used in this thesis study is based on applying to smooth of density values ρ_i obtained by the Equation 3.34 over neighboring particles. Relating to this, the smoothing function is defined as follows.

$$\hat{\rho}_i = \rho_i - \frac{\sum_{j=1}^N (\rho_i - \rho_j) W_{ij}}{\sum_{j=1}^N W_{ij}} \quad (3.39)$$

The corrected density values ($\hat{\rho}_i$), are firstly substituted into the state equations given by 3.33 to be able to obtain the pressure values and then by substituting the same corrected values for densities in Navier-Stokes equations stated in 3.35, the particle accelerations are calculated in a precise and proper manner.

3.6.3 Free Surface Correction

A numerical correction algorithm is applied to the particles which are defined as free surface (on the) boundary. This numerical correction technique prevents the particles from excessive scattering and keeps them together and a numerical correction algorithm acting like free surface tension has been applied to the particles defined as the free water surface. The same numerical algorithm provides an effect for free surface tension and mimics this phenomenon in the simulation.

According to this definition, the particles having %65 fewer number of particles than the maximum number of neighboring particles in the problem region are marked as free water surface particles.

In the studies ([84], [83]) where the severe flow problems with free water surface have been covered, the ratio corresponds to 1-2 lines of particles depending on deformations caused by flow motion. It has been shown that it is not possible to represent the free water surface realistically with smaller and bigger values of this ratio.

In this study, the free water surface is calculated through the same approach mentioned. The free water surface correction algorithm used is given by the following statement.

$$\delta \mathbf{u}_i = \frac{\sum_{j=1}^N (\mathbf{u}_i - \mathbf{u}_j) W_{ij}}{\sum_{j=1}^N W_{ij}}, \hat{\mathbf{u}}_i = \mathbf{u}_i - \epsilon \delta \mathbf{u}_i \quad (3.40)$$

where $\hat{\mathbf{u}}_i$ represents the velocities of corrected particles (the corrected velocities of particles) while ϵ is the coefficient which determines how much the distance, dx , will be between the particles in the initial state. Many investigations performed within the context of this study indicate that this ratio should be kept in the range of 0.05 – 0.10. This correction is only applied to the particles defined as the free water surface.

3.6.4 Particle Displacement Correction

Since the SPH method is based on the interpolation approach which takes place over the particles distributed in a continuous region, the particles are needed to be homogeneously distributed to be able to provide the numerical stability and increased convergence. If the particles in the problem domain have non-homogeneous distribution and accumulation of the particles takes place in local regions during the flow motion of the liquid medium, the stability of the numerical solution gets worse and relating to this, no solution can be obtained in many cases.

It has been suggested in [90] that a tiny artificial translation to be given to the position vectors of each particle in order to prevent the accumulation/clustering along a flow line.

In the pioneering study by ([84],[82],[83]), based on this correction algorithm, required updates for modeling of free water surface problems have been performed and successfully applied to many of compelling and severe flow problems. Particle translational algorithm used in this thesis study are given as follows with Δt time step in second.

$$\delta \mathbf{r}_i = \sum_{j=1}^N \frac{\mathbf{r}_{ij}}{r_{ij}^3} r_0^2 u_{cff} \Delta t \quad (3.41)$$

$$r_0 = \frac{1}{N} \sum_{j=1}^N r_{ij} \quad (3.42)$$

$$u_{cff} = |\delta \mathbf{u}_i| \quad (3.43)$$

3.7 Time Integration and Boundary Conditions

In this study, change in time for the evolution of the flow motion is evaluated by means of Euler numerical schematic including a sub-step called predictor-corrector. The effects of numerical integration schematic used in the modeling of free water surface problems over the results have been compared in detail [54]. Single-step Euler, sub-step Euler and fourth-degree Runge-Kutta time integration schematic have been systematically compared in [54]. As a result, it has been understood that the sub-step Euler is the most appropriate approach when it is evaluated in terms of stability, correctness/precision and also computational time.

The time integration schematic used in this thesis study is based on the Euler approach which includes the predictor-corrector time sub-step. In this approach, positions, densities, and velocities are updated by the following set of equations.

$$\left(\frac{d\mathbf{r}_i}{dt}\right) = \mathbf{u}_i, \left(\frac{d\rho_i}{dt}\right) = k_i, \left(\frac{d\mathbf{u}_i}{dt}\right) = \mathbf{a}_i \quad (3.44)$$

Change of physical variables over time is started by evaluation of a equations for velocities, positions and densities of the particles in the sub-step. These equations are $\mathbf{u}_i^{(n+1/2)} = \mathbf{u}_i^{(n)} + 0.5\mathbf{a}_i^{(n)}\Delta t + \delta\mathbf{u}_i^{(n)}$, $\mathbf{r}_i^{(n+1/2)} = \mathbf{r}_i^{(n)} + 0.5\mathbf{u}_i^{(n+1/2)}\Delta t + \delta\mathbf{r}_i^{(n)}$, $\rho_i^{(n+1/2)} = \rho_i^{(n)} + 0.5k_i^{(n)}\Delta t$, respectively.

After the updated densities evaluated in the sub-step is corrected by the equation given in 3.39 and evaluation of pressure values by Equation 3.33, acceleration of the particles which is represented by $\mathbf{a}_i^{(n+1/2)}$ is obtained by means of the set of equations given by 3.35 and 3.36.

Then, the velocity vector belonging to the next time step which is $\mathbf{u}_i^{(n+1)} = \mathbf{u}_i^{(n)} + \mathbf{a}_i^{(n+1/2)}\Delta t + \delta\mathbf{r}_i^{(n+1/2)}$, is evaluated by means of acceleration values obtained in the sub-step.

Then the particles moves according to $\mathbf{u}_i^{(n+1)} = \mathbf{u}_i^{(n)} + \mathbf{a}_i^{(n+1/2)}\Delta t + \delta\mathbf{r}_i^{(n+1/2)}$ in which the obtained velocity vector values are substituted. Courant-Freidrichs-Lewy(CFL) condition as a time-step criteria which is formulated by the following equation.

$$\Delta t = CFLF \left(\frac{h}{c_0 + c_d} \right) \quad (3.45)$$

where CFL is assigned to 0.1.

In the numerical calculations, the no-slip boundary condition is applied to the tank's walls. To be able to satisfy this condition in the numerical simulations, four lines of fixed particles are placed along all the wall boundaries of the tank. The reasons why four lines of particles are preferred are because the impact region of the weighting function used has a length of $3h$ and the length of interpolation length is defined as $1.33dx$. Thus, it is allowed that the particles being close to the boundaries can interact with boundary particles in their entire influence domain.



4. SPH MODELLING OF WEDGE ENTRY PROBLEM WITH CONSTANT VELOCITY AND ACCELERATION

4.1 Problem Geometry and Parameters

In this study, the water entry problem is investigated for different particle spacing and deadrise angles at a constant velocity and obtained numerical results are compared with experiment and numerical findings of the literature.

The problem domain for the wedge entry problem is demonstrated in Figure 4.1. In our current problem, the wedge is allowed to drop down from a determined drop height defined by parameter " a " which is set to $0.35m$ from the water surface. The width and height of the tank geometry are represented by L and D terms which are assigned to $2.8m$ and $1.62m$ respectively for the current model. In the wedge geometry, the distance between the keel and top of the wedge is defined by h which is $0.267m$ while the width of the wedge at the top is set to $0.718m$. Still water level indicated by H in Figure 4.1 is $1m$ while the deadrise angle is represented by θ .

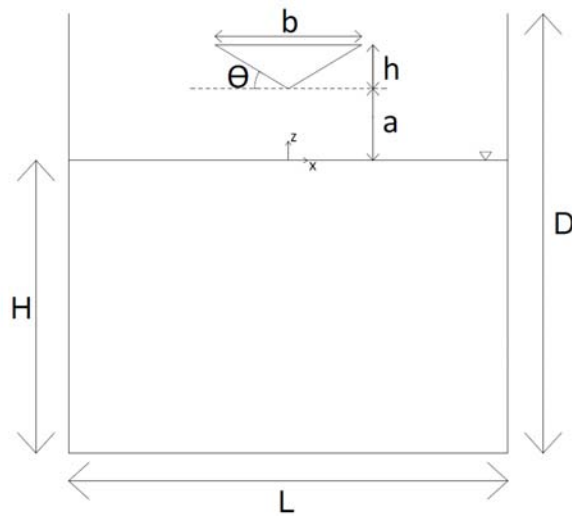


FIGURE 4.1: Schematic representation of problem geometry

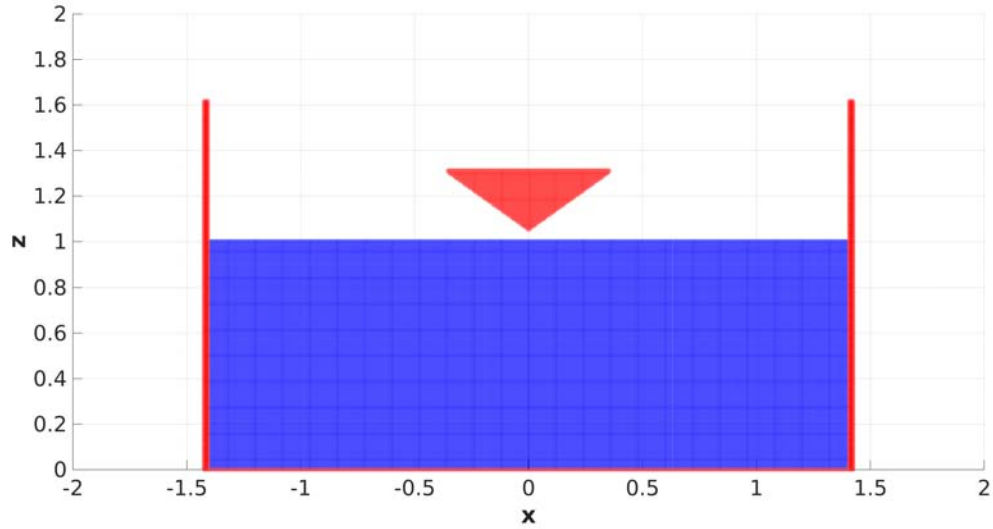


FIGURE 4.2: Schematic representation of problem geometry

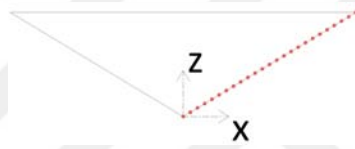


FIGURE 4.3: Representation of pressure points on the wedge

Zhao and Faltinsen et al. [107] studied on the same problem where they used boundary element method. The numerical results that are provided as an outcome of the developed model in this current study are compared with Zhao and Faltinsen et al.'s reference study [107]. For a convenient comparison of the numerical result, twenty-five pressure points as illustrated in Figure 4.3 were placed along the edge to capture the distribution with enough resolution.

As a numerical method, the SPH model developed for this specific type of problem is deployed to examine the water entry phenomenon with constant velocity case. The angle between the edge of the wedge and horizontal axis is defined as the deadrise angle and the numerical studies have been carried out to investigate the dependency of the pressure distribution to the deadrise angle. Deadrise angles specifically chosen in this current study are 30° and 35.6° .

4.2 Numerical Results of Constant Velocity

Zhao and Faltinsen et al. provided results out of their experimental and numerical studies for the constant velocity problem [107]. The results of this reference study are compared with the outcomes of this current numerical study for the same type of problem. The numerical simulation results are given below in Figures 4.5, 4.6, 4.7 and 4.8 for 35.6° deadrise angle. It should be also noted the delta distance has an effect on the pressure distribution along the edge which can be realized from difference pressure distribution trends in Figures 4.5, 4.6, 4.7 where delta distance has been chosen as $6mm$, $8mm$ and $10mm$ respectively.

In Figure 4.5a, it is shown that the pressure distribution for 35.6° deadrise angle stands between the results for 30° and 40° .

As can be seen from Figure 4.5a, there is consistency between in terms of results obtained in this current study and already exist in the literature.

Figures 4.9 and 4.10 demonstrates the results for 30° deadrise angle.

In the literature, it has been shown that the delta distance has an effect on the sensitivity of the numerical method in terms of obtained results [91]. For the purpose of demonstrating the effect of delta distance and to perform a convergence study, three different initial particle spacing values which are $6mm$, $8mm$ and $10mm$ have been chosen and compared with related studies in the literature. As can be deduced from Figure 4.11, the data points for the results of $6mm$, $8mm$ and $10mm$ particle resolutions of SPH method provides similar trendline to other studies in the literature with a good agreement. Regarding the results of SPH simulations, it can be mentioned that there is no significant distinction among pressure distributions of the test cases which have varying particle resolutions. Thus, it has been decided that further numerical analyzes should be performed by $10mm$ delta distance since the computational time costs drop remarkably with increasing initial particle spacing. A set of data including the comparison of computational time with delta distance is presented in Table 4.1. In convergence study, the last three pressure points that are placed on the top corner of the wedge have not been considered due to the lack of neighboring fluid particles that

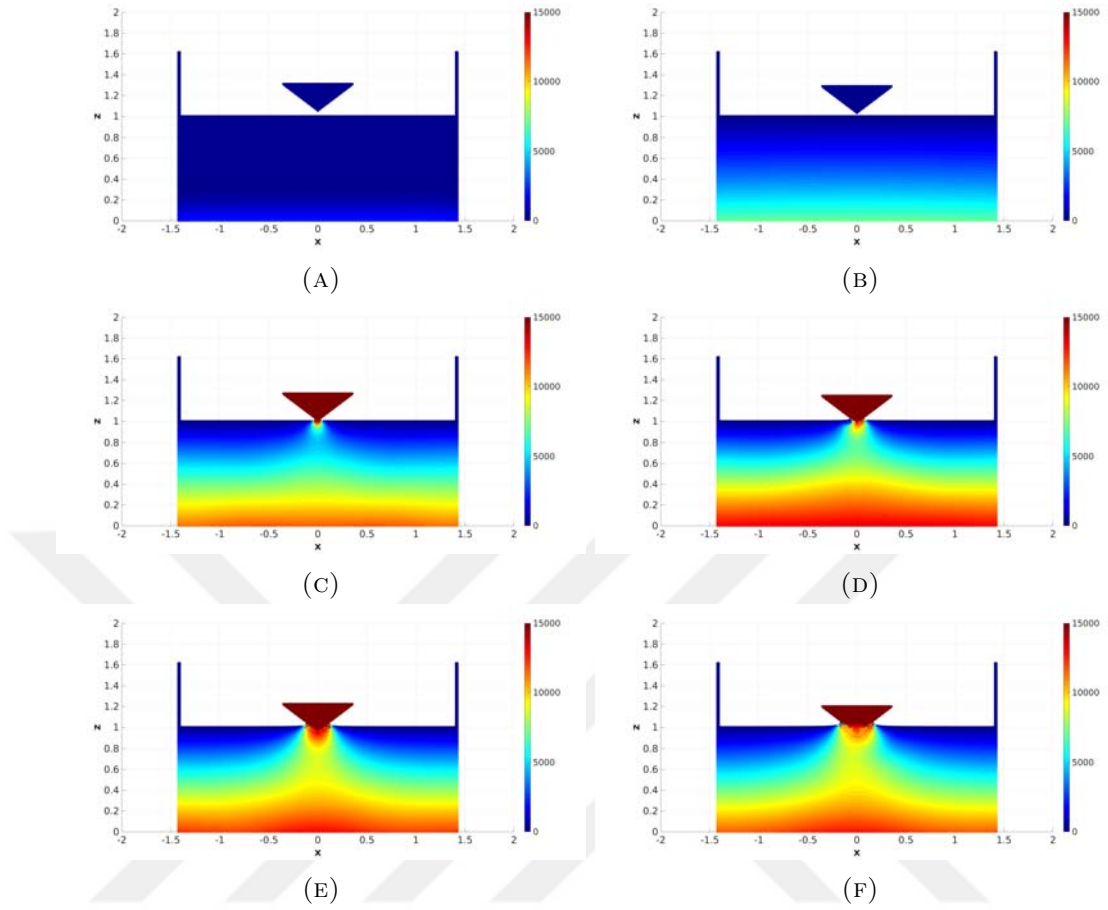
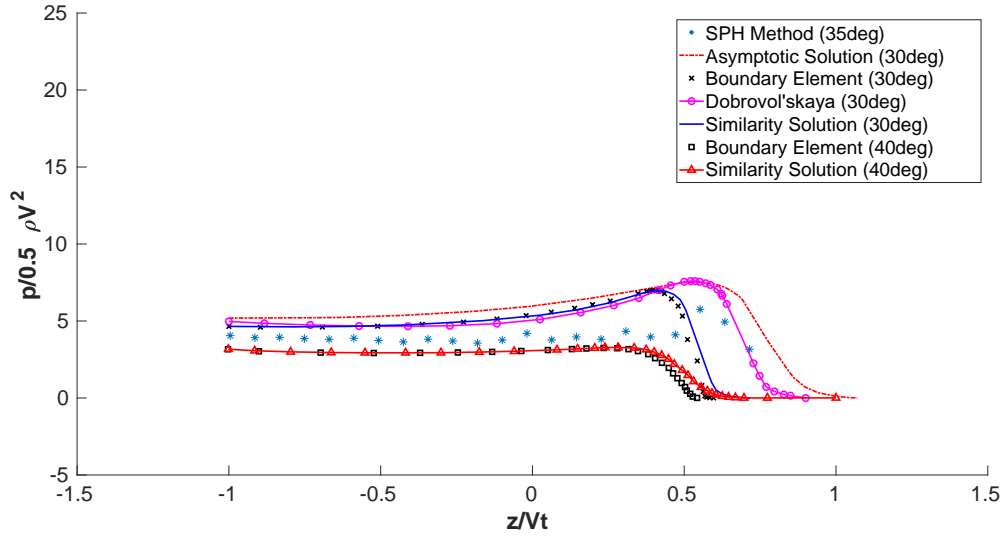


FIGURE 4.4: Falling sequence

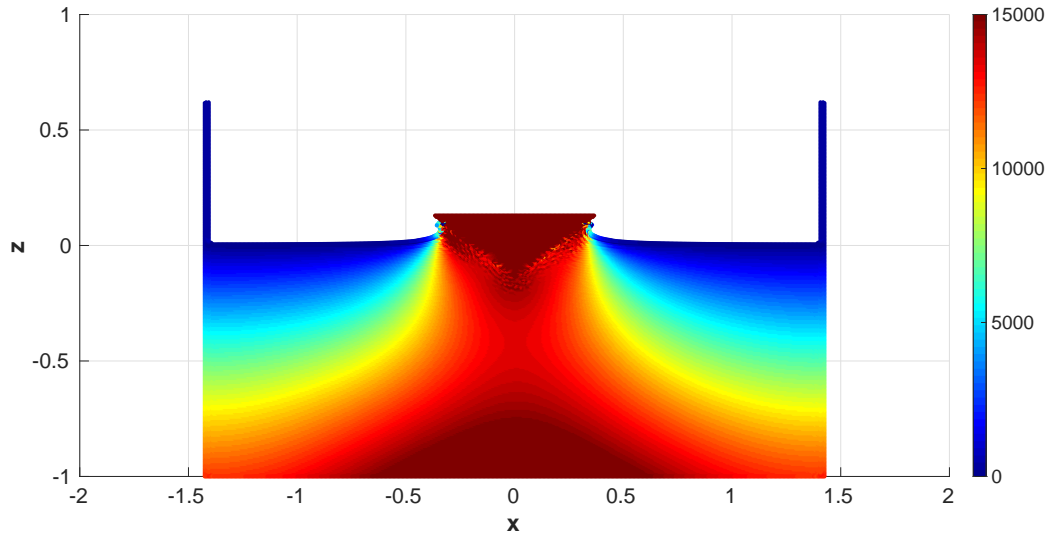
TABLE 4.1: Computational time cost per unit cycle for variable initial particle spacing

Δ [mm]	Time duration of a cycle [s]
6	9.162
8	3.450
10	1.638

yield unphysical pressure beats. From a physical point of view, the pressure values at these points decline suddenly and approach zero.



(A) Pressure distribution

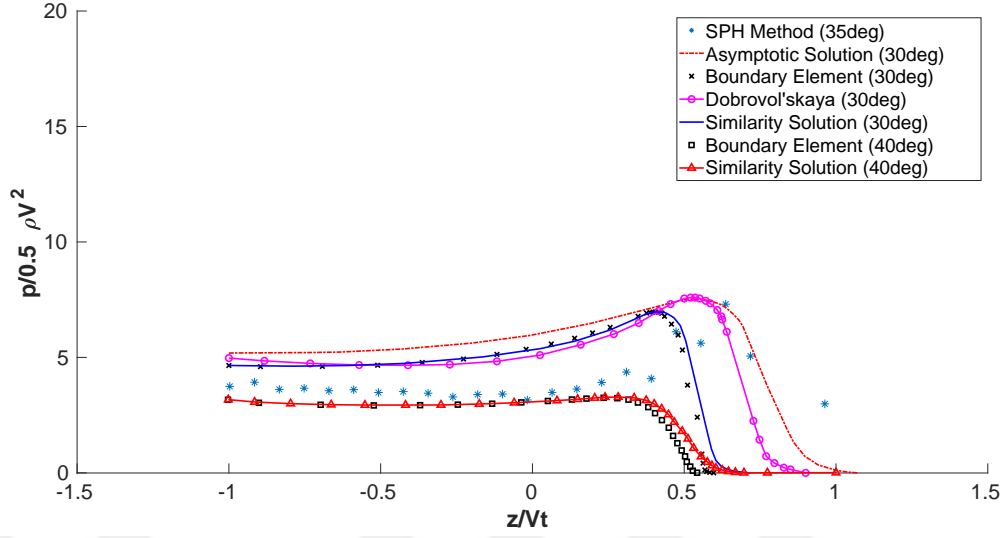


(B) Pressure field [Pa]

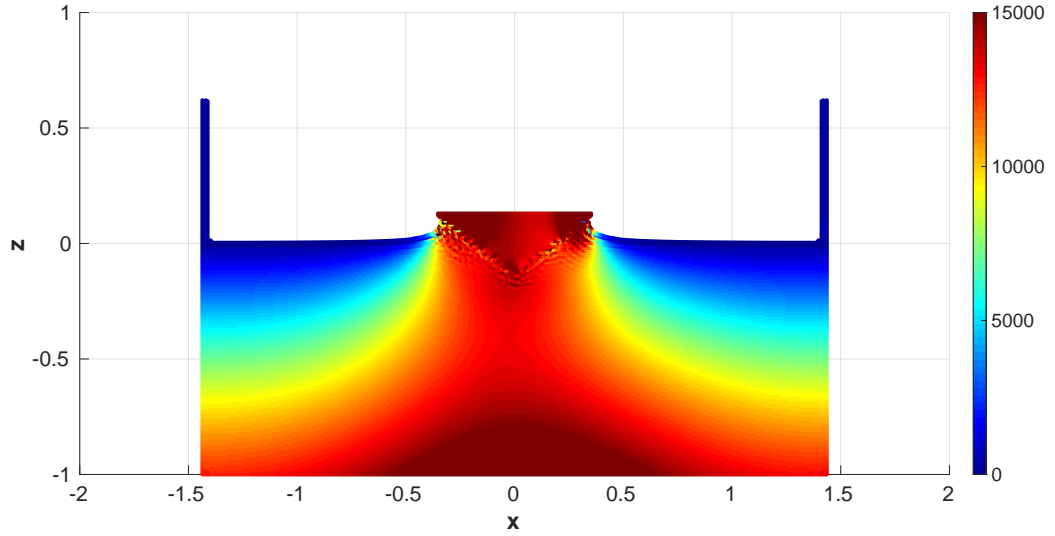
FIGURE 4.5: 35 degree, $t=0.073s$, $\delta=6mm$

4.3 Viscous Penalty Treatment in SPH Scheme

When a wedge-shaped body moves in calm water, some interactions occur between fluid and solid phases because of the viscosity ratio between wedge and water. In order to improve the previously obtained numerical results in this study, SPH method calculations have been modified. The modification that has been implemented in the SPH method is called viscous penalty (VP) scheme which increases viscous diffusion in the Navier-Stokes equation and carries out rigid-body motion in a fluid.



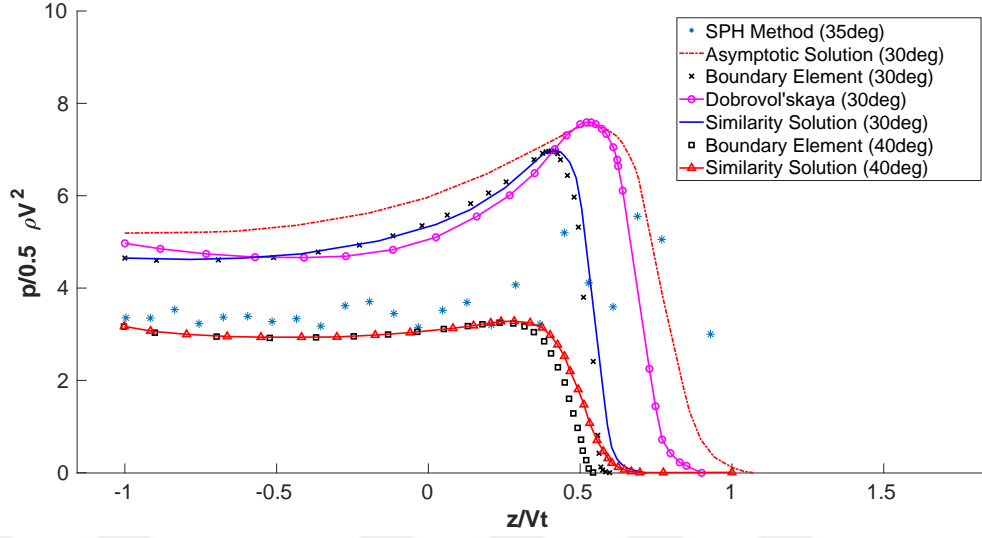
(A) Pressure distribution



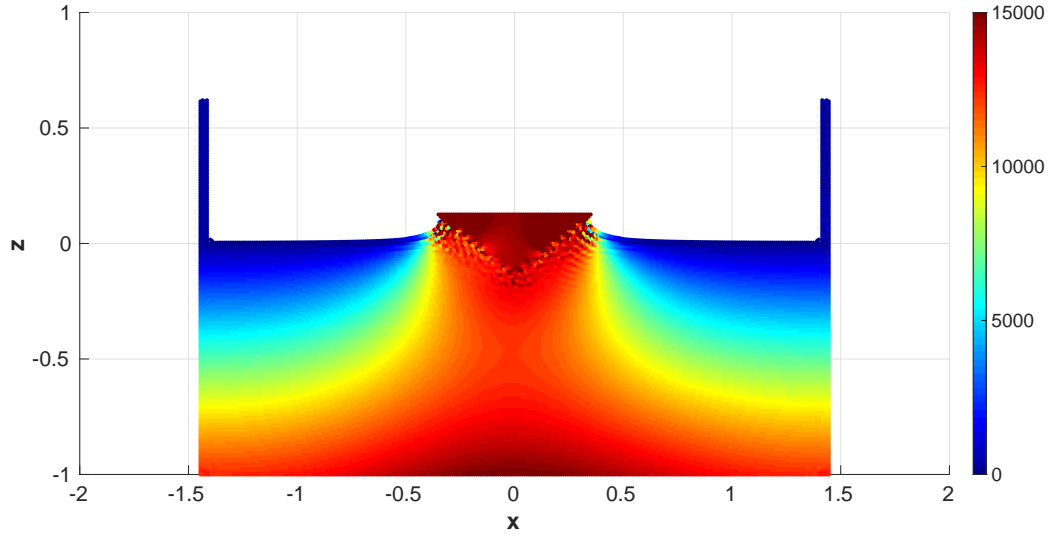
(B) Pressure field [Pa]

FIGURE 4.6: 35 degree, $t=0.079s$, $\delta=8mm$

Because of solid-liquid or liquid-liquid interactions, the boundaries of different phases should be discriminated all along with the analysis. The reason for that, a mathematical description called color function is stated to recognize the phases associated with different liquids and solid media in the problem. The color function defined by \hat{c}^α is assigned either to unity or zero depending on which phase it represents. Smoothed form of the color function for the particles along the phase boundaries which are interacting with its neighbors is stated as



(A) Pressure distribution

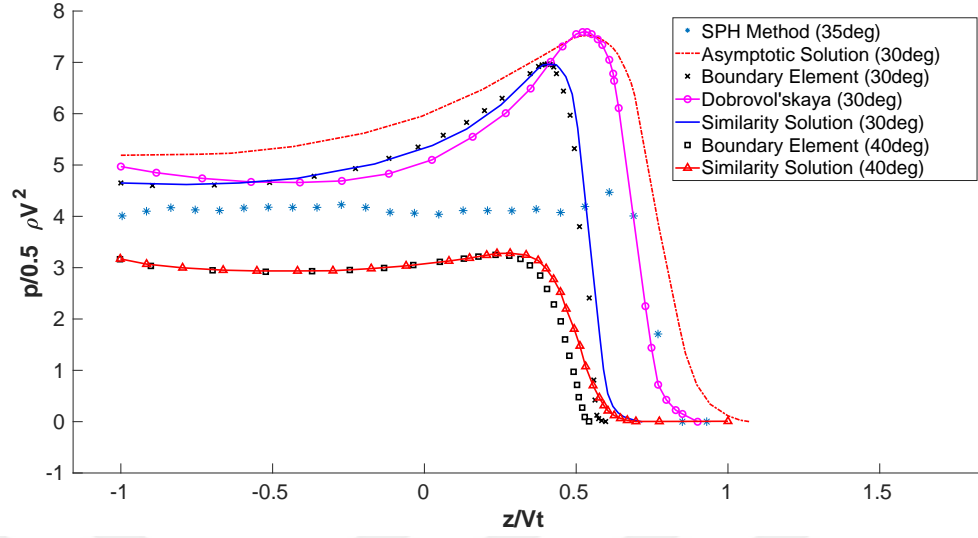


(B) Pressure field [Pa]

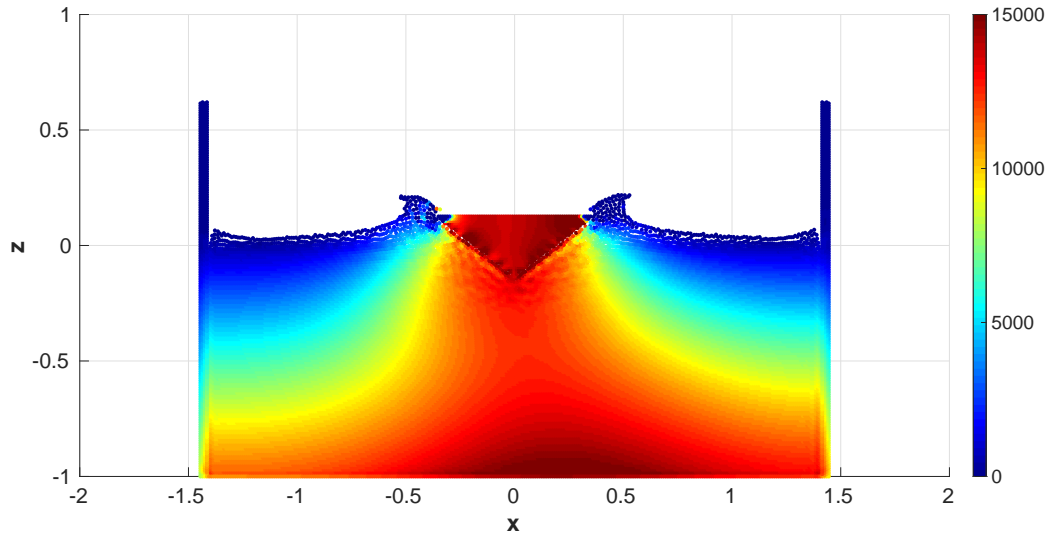
FIGURE 4.7: 35 degree, $t=0.085s$, $\delta=10mm$

$$c_i^\alpha = \frac{1}{i} \sum_{j=1}^{J_n} \hat{c}_j^\alpha W_{ij} \quad (4.1)$$

Hereby, the kernel function is utilized to provide the smoothness of the quantitative values for physical properties in the interpolation of phases. In Equation 4.1, the shortened notation W_{ij} is used to represent interpolation kernel $W(r_{ij}, h)$ which is defined as a function of magnitude for distance vector between the interacting particles, $r_{ij} = r_i - r_j$ and smoothing length, h which is assigned to a value that is 1.33 times



(A) Pressure distribution

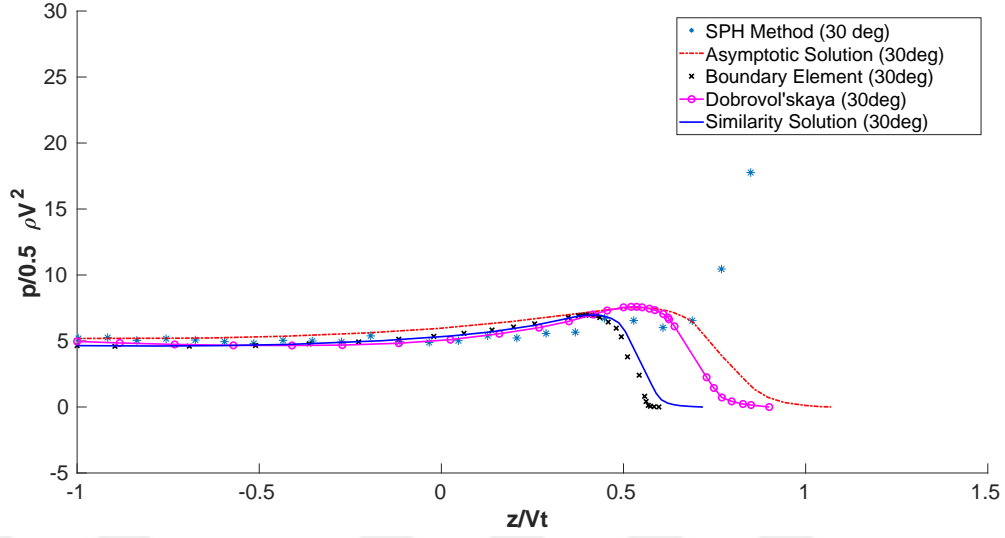


(B) Pressure field [Pa]

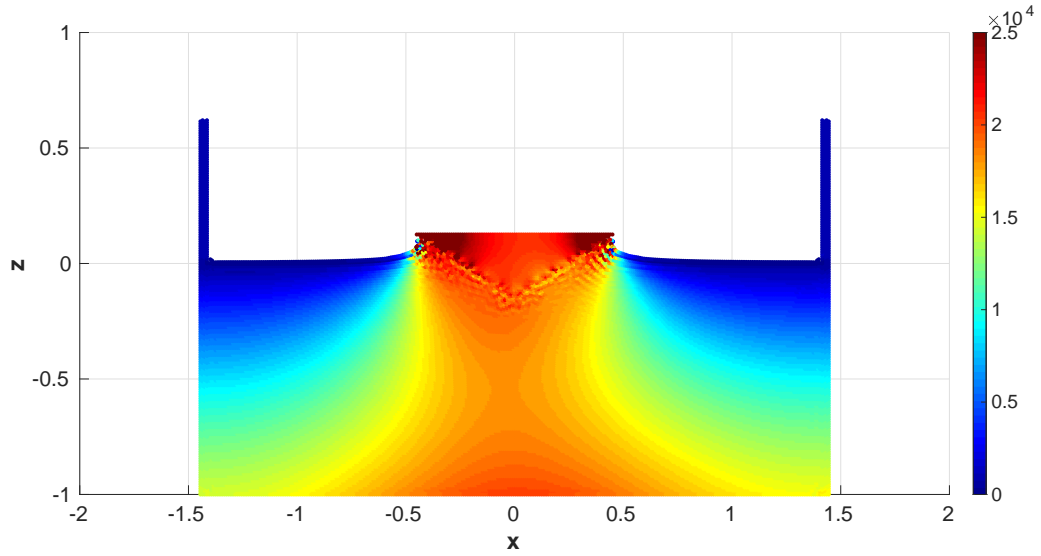
FIGURE 4.8: 35 degree, $t=0.085s$, $\delta=10mm$, $h=2mm$

longer than the separation distance at the initial state. The number density of the particle of the interest interacting with its surroundings is calculated as

$$\psi_i = \sum_{j=1}^{J_n} W_{ij} \quad (4.2)$$



(A) Pressure distribution



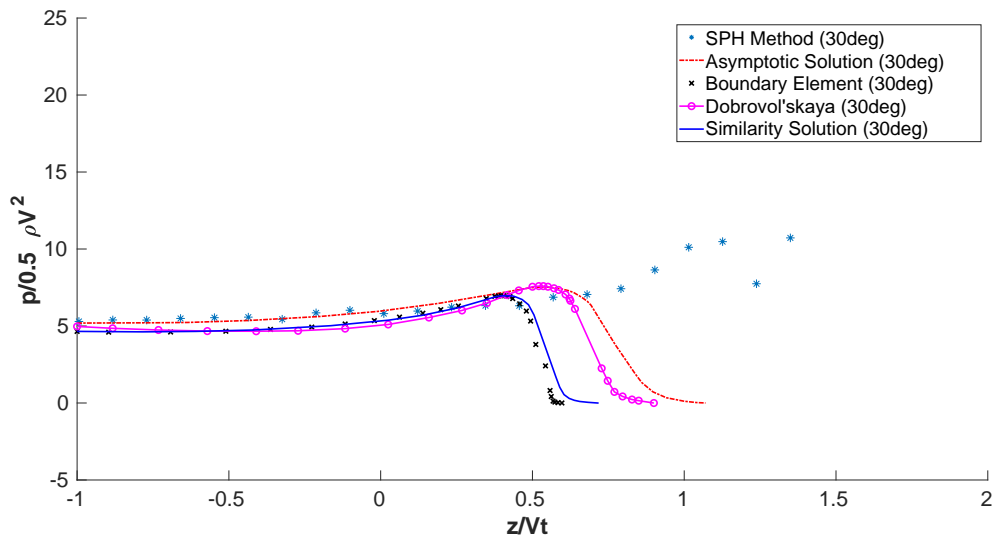
(B) Pressure field [Pa]

FIGURE 4.9: 30 degree, $t=0.085s$, $\delta=10mm$, $h=1.33mm$

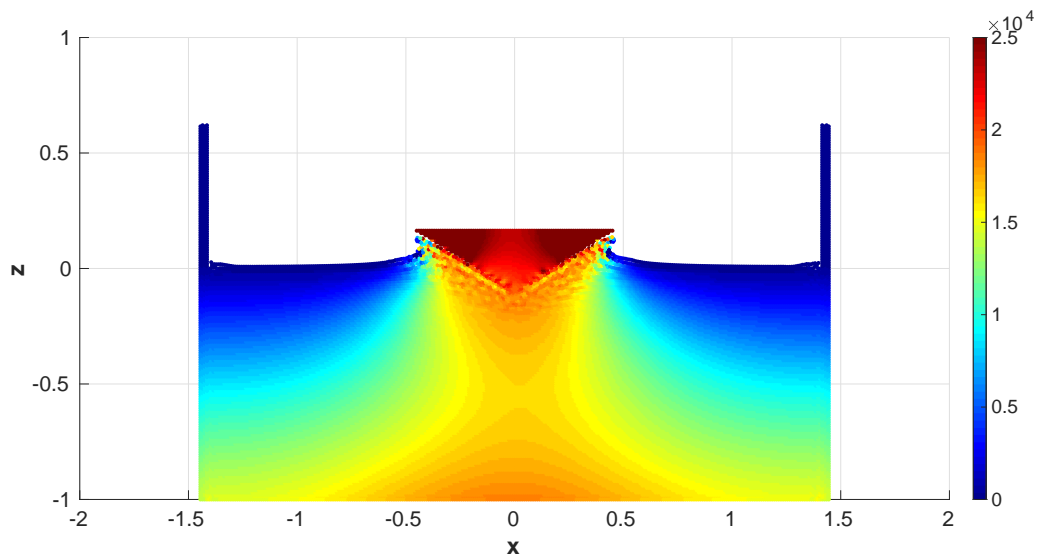
Transition region having the compact support distance of quintic kernel function between two phases is obtained which is assigned to three smoothing lengths ($3h$).

A weighted harmonic mean(WHM) is defined to compute interpolations of phase properties of a single fluid phase for c_i and other multiple solid phases as

$$\frac{1}{\mu_i} = \sum_{\alpha} \frac{c_i^{\alpha}}{\mu_s^{\alpha}} + \frac{c_i}{\mu_f} \quad (4.3)$$



(A) Pressure distribution



(B) Pressure field [Pa]

FIGURE 4.10: 30 degree, $t=0.070s$, $\delta=10mm$, $h=1.6mm$

where the viscosity of interested particle can be represented by term μ when needed to calculate. Treating solid phase as a rigid body is performed by assigning its viscosity to higher values.

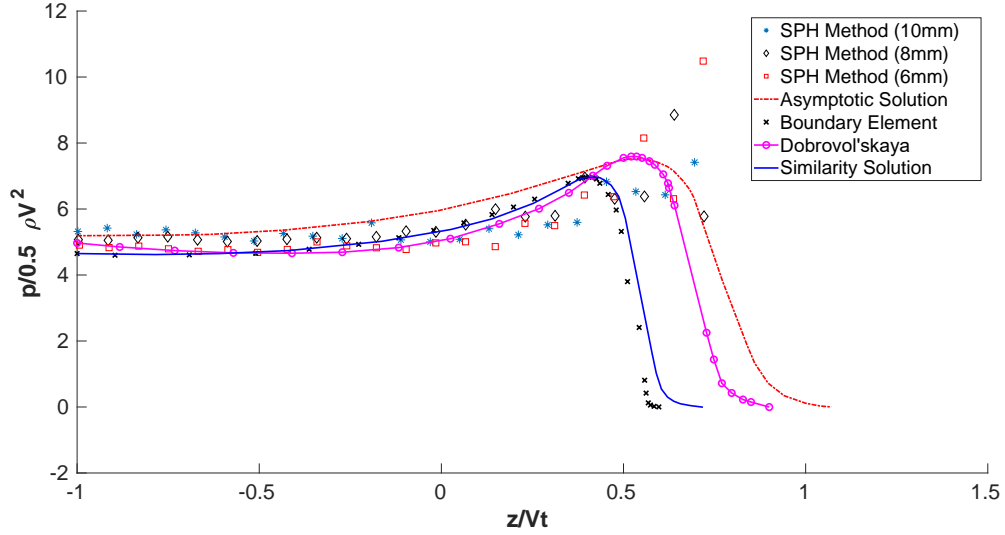


FIGURE 4.11: Comparison of pressure distribution

4.3.1 SPH Results with Viscous Penalty Method

Results in the current literature are compared with the outcomes of the VP implemented SPH method, and outcomes of the classical SPH approach separately in different plots. A comparison of the outcomes based on SPH with VP implementation for $6mm$, $8mm$ and $10mm$ particle resolutions and literature results is presented in Figure 4.12. As it can be deduced from Figures 4.13, 4.14 and 4.15, it is frankly seen that oscillating data of the classical SPH method diminishes and becomes more stable when the VP treatment is implemented in the classical SPH method.

4.4 Numerical Results of Constant Acceleration

In this section, VP implemented the SPH method is enriched with the addition of a fluid-solid interaction(FSI) algorithm which is going to be further explained in the following section. Before starting the free-fall problem where further analyzes will be tested in real terms based on our FSI algorithm, simulations are performed with a constant acceleration of a wedge body (neglecting the buoyancy force acting on the body from the moment of impact) and obtained results are compared with

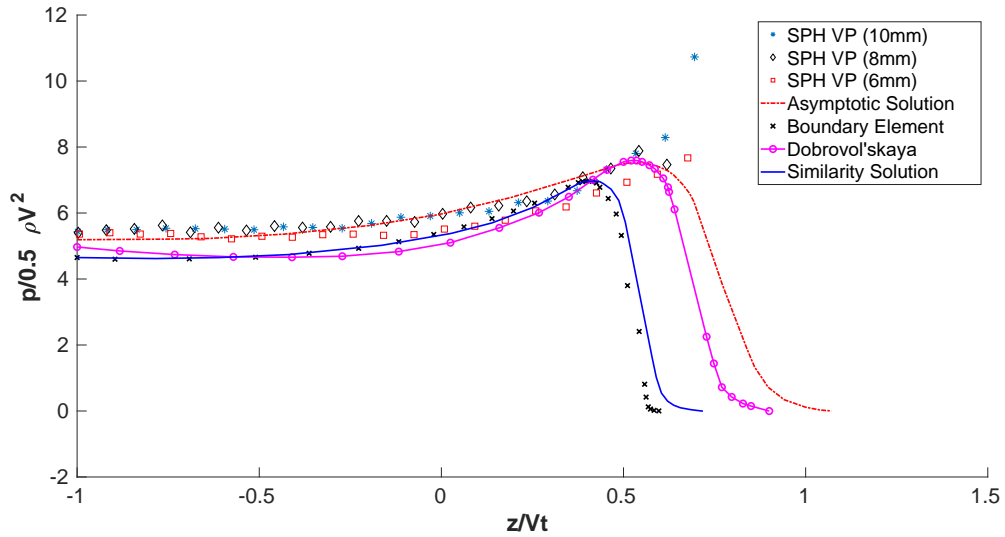


FIGURE 4.12: Comparison of pressure distribution with VP method

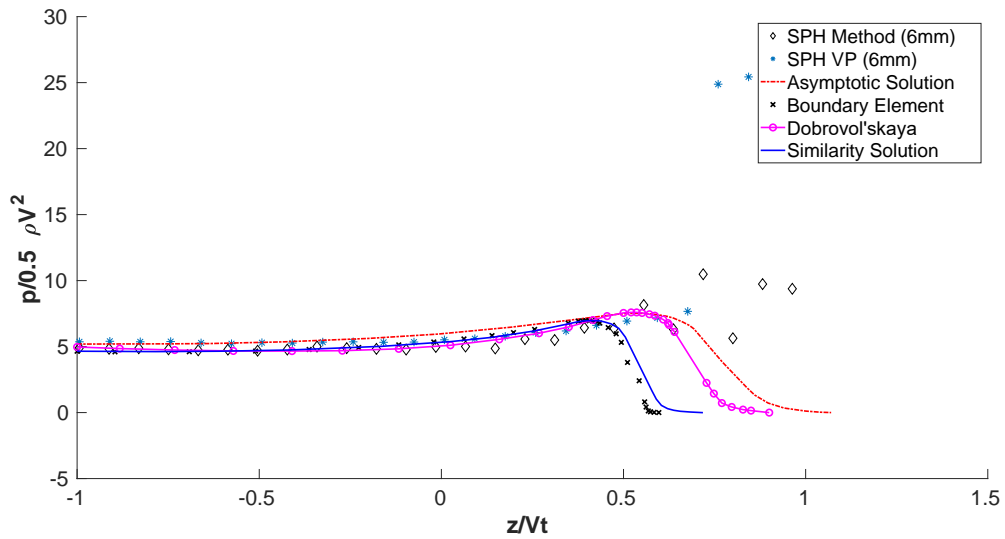


FIGURE 4.13: SPH method vs VP method (6mm)

the experimental/numerical results proposed by Zhirong et al. [108] for the free-fall problem.

Figure 5.1 gives the location of the pressure sensors on the object (Zhirong et al.[108]). As seen on the figure the wedge body, which the reference work defines as Model I, has a curvature from the point of the pressure sensor P1. In order to express this curvature geometrically, coordinates of several points are required in the curvature region. By neglecting this small geometric difference, three pressure sensor

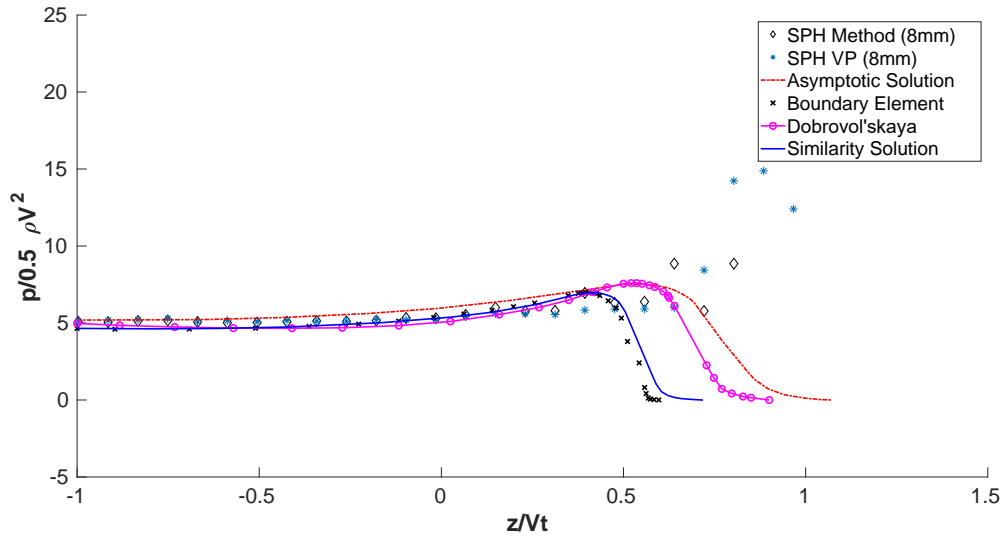


FIGURE 4.14: SPH method vs VP method (8mm)

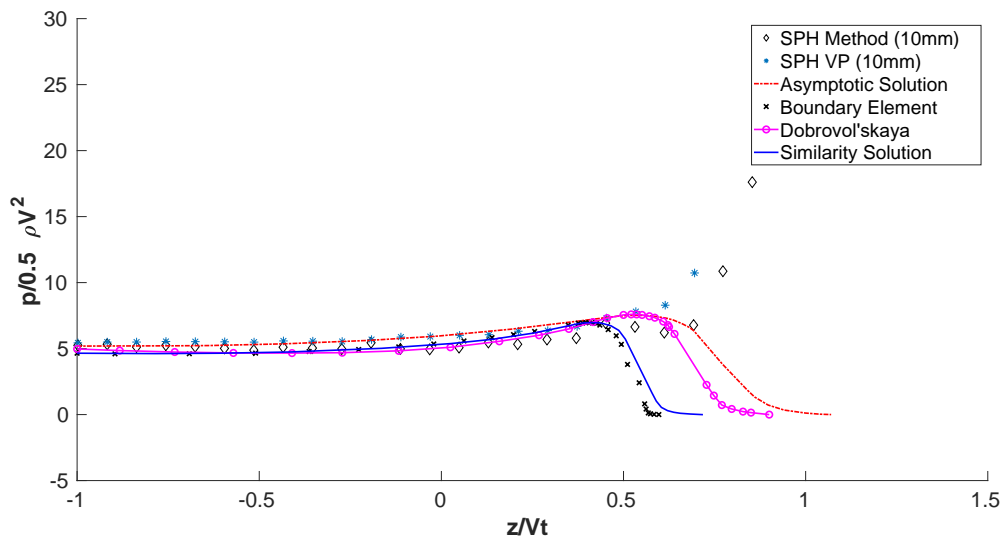


FIGURE 4.15: SPH method vs VP method (10mm)

points were passed through a line and simulations are performed by forming a wedge as shown in magenta.

In Figures 4.16 and 4.17, the position and velocity time series of the wedge body and also the pressure readings at the pressure measurement points are given. $t = 0$ indicates the moment when the keel of the wedge comes into contact with water. This simulation is performed by taking the delta distance as 10mm.

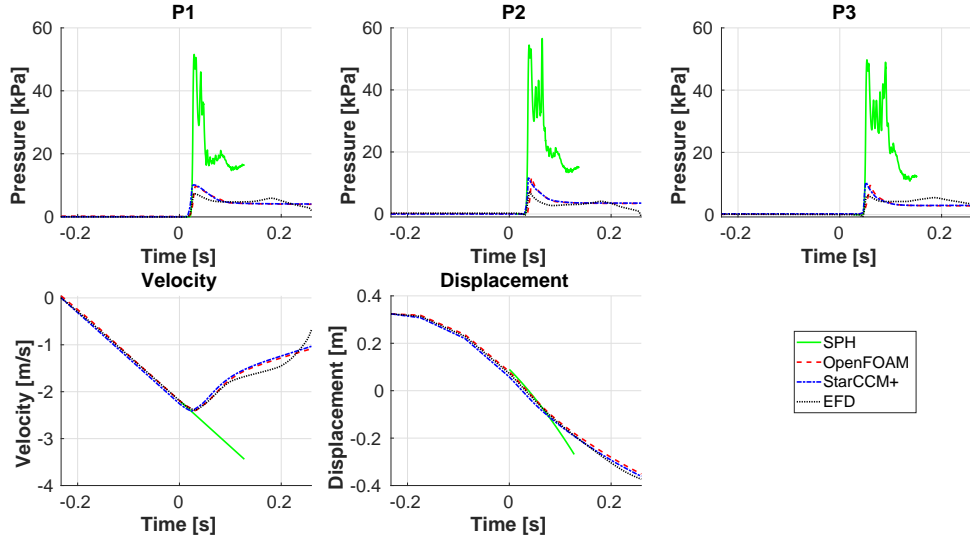


FIGURE 4.16: Change in displacement, the velocity of the wedge body and pressure values captured from sensor points for 10mm delta distance with constant acceleration

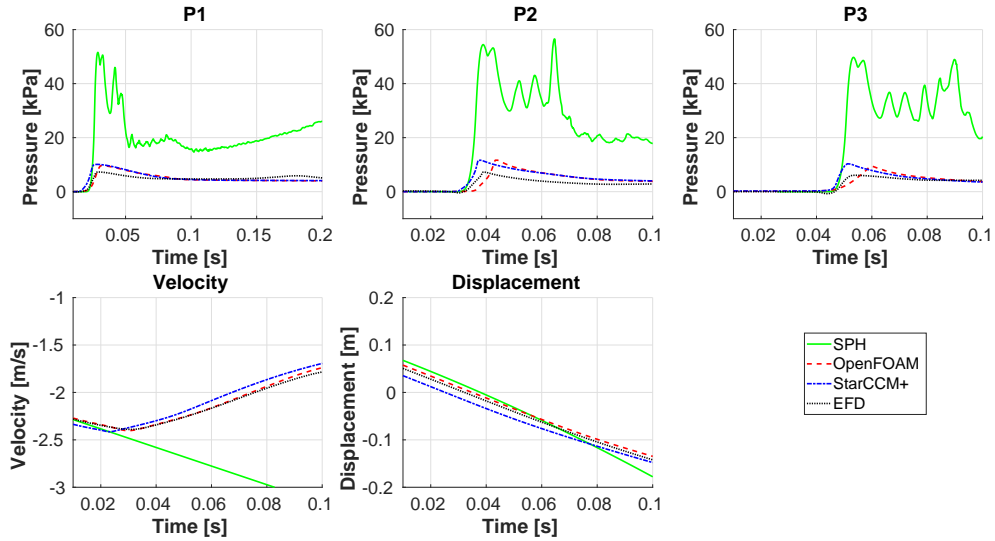


FIGURE 4.17: Change in displacement, the velocity of the wedge body and pressure values captured from sensor points for 10mm delta distance with constant acceleration-a close-up view after the moment of impact

Displacement time series of Figure 4.16 reveals that there is a distinctive correlation in terms of the results when numerical and experimental studies are investigated along 0.08s after the impact instant. Moreover, according to the reference study, the velocity-time graph in Figure 4.16 shows that the buoyancy force applied on the wedge body becomes effective 0.025s after the collision event happens. The velocity of the body after the impact diminishes in time. As opposed to this, the velocity of the wedge

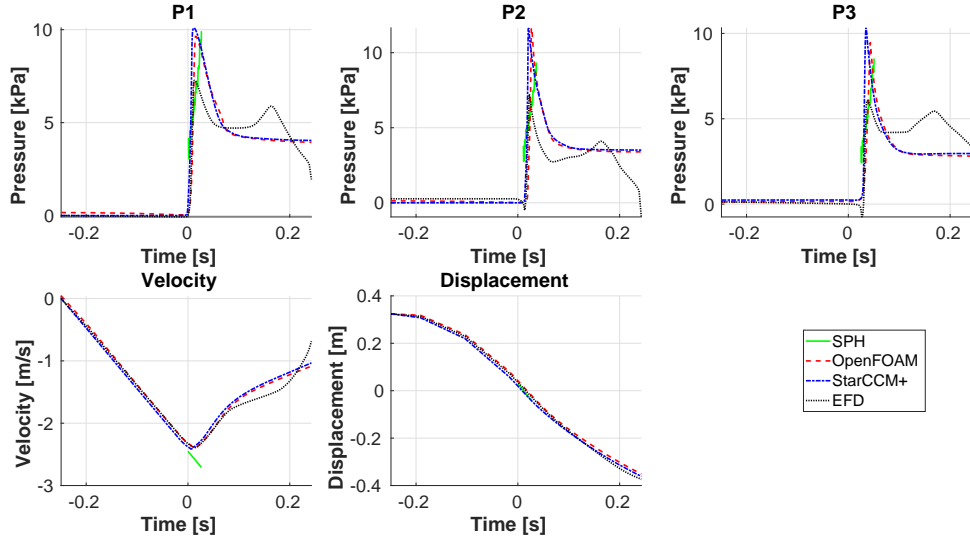


FIGURE 4.18: Change in displacement, the velocity of the wedge body and pressure values captured from sensor points for 6mm delta distance with constant acceleration

body increases in time because it moves with constant acceleration during its all motion in the SPH simulation. This situation causes the wedge body to experience higher pressure values than it is supposed to be in comparison to the reference study. Impact instant can be distinguished in detail from the close-up views in Figure 4.17.

In order to improve the sensitivity of SPH results, initial delta distance is reduced to $6mm$. Subsequently, an additional simulation of which numerical results are provided in Figure 4.18 is once more run until the sensors detected the pressures caused by the first impact since further step after the impact do not provide meaningful outcomes because of free-fall motion of the body with constant acceleration. As a conclusion obtained numerical outcomes of simulation with $6mm$ delta distance show that more compatible results compared to experimental investigations are found. In Figures 4.18 and 4.19, the position and velocity time series of the wedge body, as well as pressure readings at the pressure measurement points, are given in fullscale and close-up views respectively.

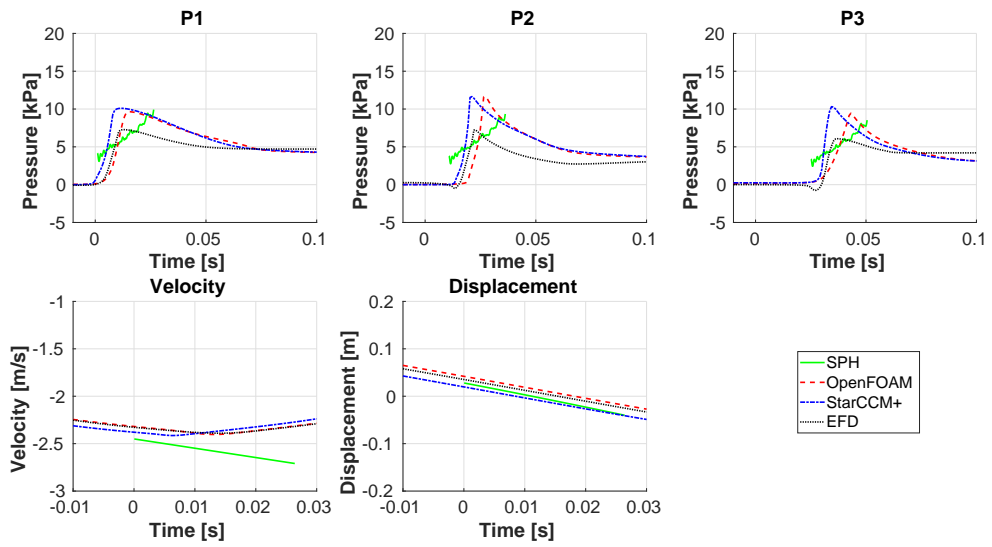


FIGURE 4.19: Change in displacement, the velocity of the wedge body and pressure values captured from sensor points for 6mm delta distance with constant acceleration - a close-up view after the moment of impact

5. SPH MODELING OF WEDGE ENTRY PROBLEM WITH FREE FALL

5.1 Problem Geometry and Parameters

At this part of the thesis study, time series of pressure distribution on a wedge-shaped body is investigated to capture the free-fall movement of the wedge block hitting still water surface. The results that are provided in the associated studies in the current literature are considered as reference and compared with the obtained numerical results in this thesis study.

Schematic representation of the problem domain and geometric parameters are kept the same as in Chapter 4, see Figure 4.1. In the numerical scheme of the SPH method, since computing time of the problem highly relies on the number of particles defined in the problem domain, numerical simulations are decided to perform with a fewer number of fluid particles. This is provided by reducing the calm water level to half of the full height defined in Figure 4.1. For this purpose, calm water heights are assigned to $1m$ and $0.5m$ respectively. Deadrise angle which is set to 35.6° and 37.3° .

Comparison of the obtained results is provided based on a reference study by Zhirong et al. [108]. For the purpose of convenient comparison, three pressure points are placed along the wedge boundary as illustrated in Figure 5.1.

5.1.1 Fluid–Solid Interaction Algorithm

The diffusion of the solid particles towards the liquid phase occurs in the interface domain because of the considerable difference in viscosities assigned to the solid and liquid phases. An additional treatment is needed to keep the solid particles together whose support domain includes particles in the fluid phase since surrounding fluid particles cause deficit viscosity and taking solid particles apart from the rigid body.

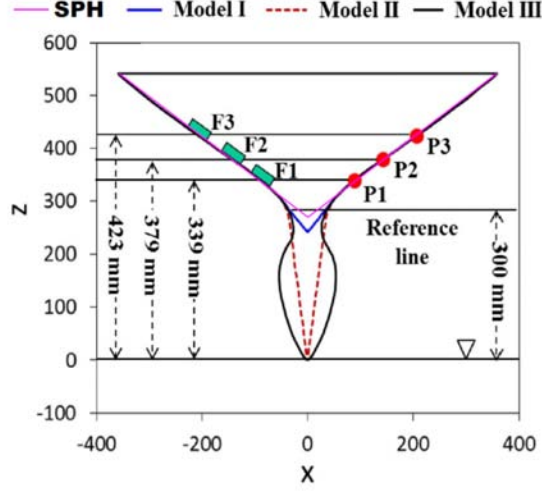


FIGURE 5.1: Schematic representation of problem geometry

To be able to allow solid particles to constitute a solid body, further treatment has been developed including constraints based on conservation of momenta [55]. These constraints utilize from the calculation of the momentary velocities of the solid particles for determining of the center of mass and angular velocities of the solid body. Terms that are associated with angular velocity and center of mass are calculated by means the formulations given below.

$$u_s^r = \frac{1}{I_s} \sum_{j=1}^{J_s} \frac{u_j \times r_{js}}{j} \quad (5.1)$$

and

$$u_s^t = \frac{1}{M_s} \sum_{j=1}^{J_s} \frac{u_j}{j} \quad (5.2)$$

respectively. Combining the Equation 5.2 and Equation 5.1 in rigid body formulation leads to

$$u_i = u_s^t + u_s^r \times r_{is} \quad (5.3)$$

where r_s represents the center of mass for the solid object while J_s stands for the total number of solid-phase particles. It should be also noted that the vector defined by r_{is} is the difference between r_i and r_s vectors, namely $r_{is} = r_i - r_s$. Volume and moment of inertia around the center of mass of the solid object denoted by M_s and I_s are computed by

$$M_s = \sum_{j=1}^{J_s} \frac{1}{j} \quad (5.4)$$

and

$$I_s = \sum_{j=1}^{J_s} \frac{r_{js}^2}{j} \quad (5.5)$$

respectively. In the SPH method, the method by which solid particles constitute rigid behavior as a body is to combine the viscous penalty and rigidity constraint. Rigidity constraint also provides a condition by which relative positions of the particles inside the solid phase are fixed specifically for regions where viscosity transition is large. In a conclusion, the further treatment for the implementation of solid-fluid interaction to the SPH method requires additional computational effort while application of explicit boundary condition to the scheme is eliminated.

5.2 Numerical Results

Experimental measurements are carried out on a three-dimensional object by Zhirong et al. It is found that the density of the three-dimensional object that was used in these experiments was approximately $1676 [kg/m^3]$. In the numerical analyses carried out in this thesis, solid particles are treated as the same liquid particles and the particle reference density value is defined as $1000 [kg/m^3]$. Distance between particles is taken $10mm$.

During the free-fall motion of the wedge body with 35.6° deadrise angle, pressure values read from the sensors positioned as demonstrated in Figure 5.1 and change in displacement and velocity with respect to time are presented in Figure 5.2. Due to the fact that the wedge boundary investigated in the numerical study by Zhirong et al. [108] is slightly curved towards its keel, the deadrise angle is decided to be approximated as 37.3° and numerical results have been obtained accordingly.

When Figure 5.2 and Figure 5.3 are examined it is noticed that the pressure at the impact instant decreases with increase in deadrise angle.

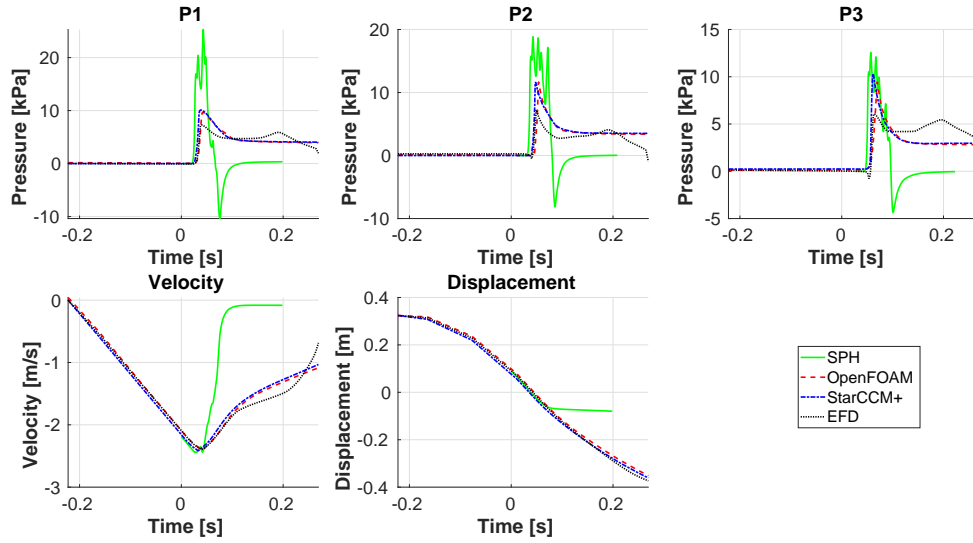


FIGURE 5.2: Change in displacement, the velocity of the wedge body and pressure values captured from sensor points for 35.6° deadrise angle, $H=1.0m$, $a=0.324m$

The results for 37.3° deadrise angle and water level height being $0.5m$ are given in Figure 5.4, where water level indicated by H , is halved to reduce computational time in numerical analyzes. By doing this, the total number of particles is reduced to 14100 in comparison to the full-scale problem domain including 28200 particles.

When Figure 5.4 and Figure 5.3 are compared, no distinction has been observed in terms of obtained results, therefore, the rest of the numerical analyzes are performed by assigning water level height to $0.5m$ hereafter.

It has been observed that the ultimate velocity of the wedge body by using SPH method for its free-fall motion is inconsistent with the results of the associated studies

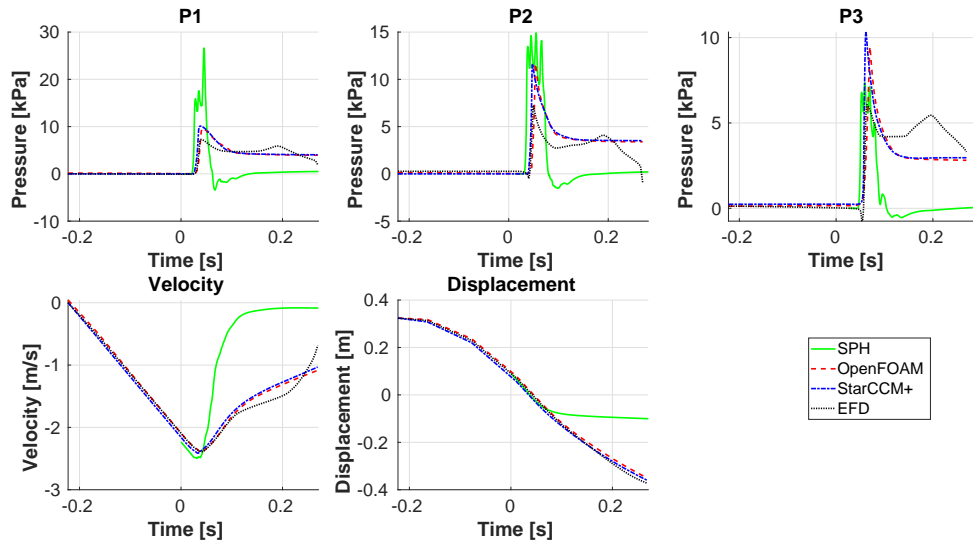


FIGURE 5.3: Change in displacement, the velocity of the wedge body and pressure values captured from sensor points for 37.3° deadrise angle, H=1.0m, a=0.334m

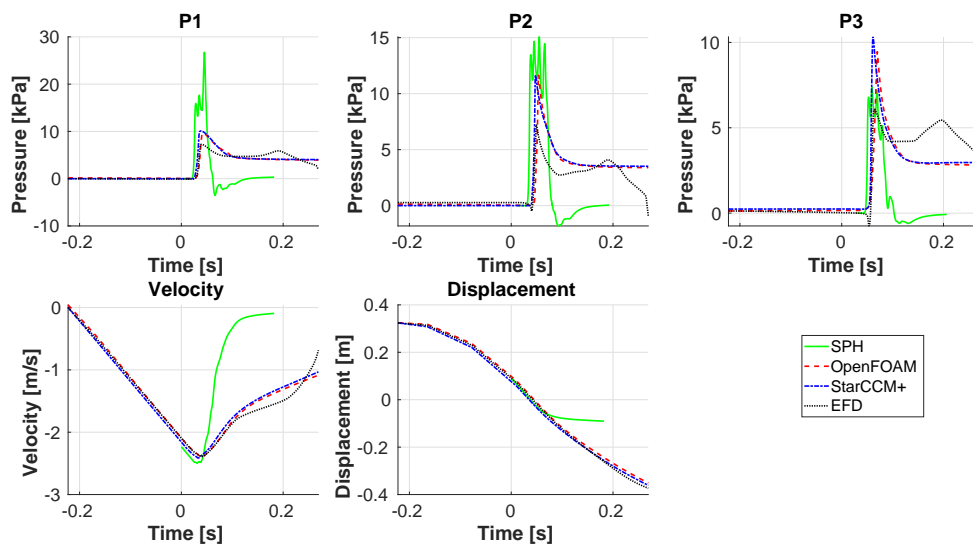


FIGURE 5.4: Change in displacement, the velocity of the wedge body and pressure values captured from sensor points for 37.3° deadrise angle, H=0.5m, a=0.334m

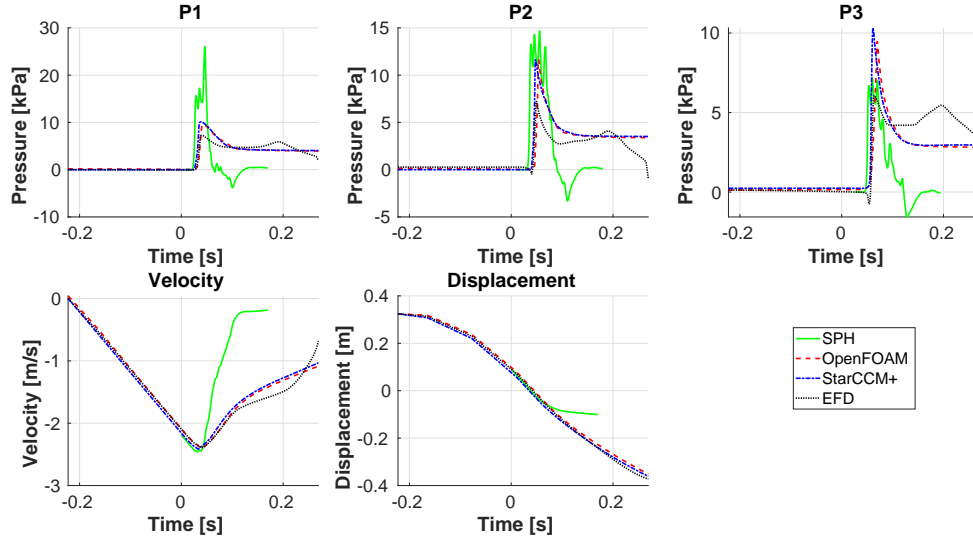


FIGURE 5.5: Change in displacement, the velocity of the wedge body and pressure values captured from sensor points for 37.3° deadrise angle, $H=0.5m$, $a=0.324m$

in the current literature [108]. The reason why a difference in ultimate velocities is observed arises from the approximation of the keel boundary to the model that is preferred to use in this current numerical study.

Numerical analysis is once more repeated to be able to obtain the same ultimate velocity value as observed in the study of Zhirong et al. [108]. In relation to this, drop height is reduced from $a = 0.334m$ to $a = 0.324m$ and the results for the drop height, $a = 0.324m$, is presented in Figure 5.5 as keeping calm water level and deadrise angle which are $H = 0.5m$ and $\theta = 37.3^\circ$ respectively. According to Figure 5.5, similar trends are noticed in terms of the results of the reference study by Zhirong et al. [108] and the SPH model provided. Therefore, in the following simulations, drop height, a , is decided to be chosen as $0.324m$.

Then, the deadrise angle was taken as 36.8° and 37° in order to examine the pressure changes corresponding to different angle values and obtained results can be seen in Figure 5.6 and Figure 5.7 respectively. By doing this, it is aimed to see how pressure values change depending on the deadrise angle in a wide spectrum.

When the plots presented in Figure 5.3, Figure 5.5, Figure 5.6 and Figure 5.7 corresponding to deadrise angles 35.6° , 37.3° , 36.8° and 37° respectively are examined, it is realised that pressure values decrease with increase in the deadrise angle.

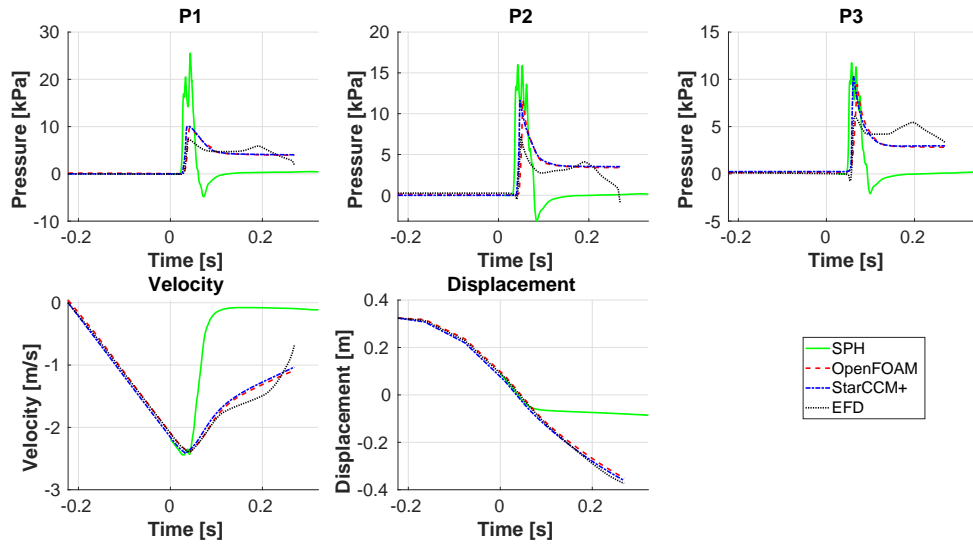


FIGURE 5.6: Change in displacement, the velocity of the wedge body and pressure values captured from sensor points for 36.8° deadrise angle, $H=0.5\text{m}$, $a=0.324\text{m}$

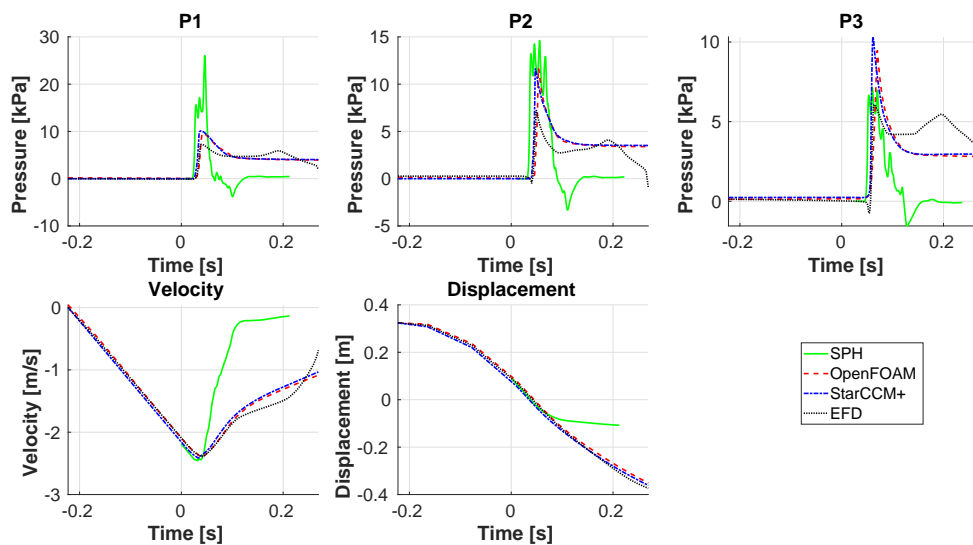


FIGURE 5.7: Change in displacement, the velocity of the wedge body and pressure values captured from sensor points for 37° deadrise angle, $H=0.5\text{m}$, $a=0.324\text{m}$

Besides, when time series belonging to pressure points indicated by $P1$, $P2$ and $P3$ are investigated it is clearly realized that the pressure values proposed in Zhirong et al.'s study [108] are lower than the observed values based on the current SPH model. Consequently, it is recommended that the delta distance between the particles shall be less than $10mm$ in the numerical scheme of the current SPH model. In this way, numerical results are supposed to approach to experimental results proposed by Zhirong et al. [108].

As a general remark, when displacement and velocity trends are observed for all the cases presented in this chapter, it is clearly seen that the net forces applied on the wedge bodies are quite distinct based on the results of the SPH method in comparison to the experimental study of Zhirong et al.[108]. Because density values of the solid phases are the same with the water, this leads the wedge body to immerse less into the liquid phase in a short time and then it starts losing its energy, as a result, velocity values immediately converge to a stable value in the results belonging to the SPH method.

6. CONCLUDING REMARKS

A two-dimensional WCSPH model has been developed to study the water entry of a wedge body with constant velocity, constant acceleration, and free-falling motion. For these three cases, pressure distributions are obtained through the sensor points placed on the wedge side and the numerical results based on the developed WSPH method are compared with other associated studies in the literature.

Based on unitless term z/Vt , for the constant velocity case of the wedge water entry problem, it is concluded that the pressures on the wedge boundary caused by slamming motion generally well agree with findings in the literature. After the implementation of VP treatment in the SPH algorithm, more stable numerical results are obtained, concluding that VP treatment provides discrimination of the phases for interacting particles. It is noted that consistent results with the literature for deadrise angles ranging from 30° to 40° are obtained.

Before the FSI algorithm is applied, the SPH algorithm developed for the constant velocity case is adapted to solve the wedge water entry problem with constant acceleration. The general trend of the pressure-time series on the sensor points shows the same characteristics with the results of associated studies in the literature. However, the amplitudes of peak pressures read from the sensor points are higher compared to others. As a result, it is concluded that this deviation is associated with continuous acceleration of the wedge body even after its engagement in calm water.

FSI algorithm is implemented in the SPH scheme for free fall simulations of wedge water entry problems.

In order to be able to provide a compatible comparison, a boundary of the wedge body is approximated to the one that in terms of its boundary because of uncertainties regarding wedge geometry in the reference study

Because of uncertainties regarding boundary of the wedge geometry in the reference study, an approximated wedge model with various deadrise angles are determined and consequently decided to use in the SPH simulations.

Consequently, obtained results out of the analyzes performed with $10mm$ delta distance provide the same characteristic trend with reference studies in the literature, however, deviations are observed in terms of peak pressures.

Besides, when time series belonging to pressure points indicated by $P1$, $P2$ and $P3$ are investigated it is clearly realized that the pressure values proposed in Zhirong et al.'s study [108] are lower than the observed values based on the current SPH model. Consequently, for future work, it is recommended that the delta distance between the particles should be chosen less than $10mm$ for convergent results in experimental investigations.

In future studies, a wedge body of which geometric parameters are known can be determined and the developed WCSPH algorithm can be validated based on the results to be obtained.

REFERENCES

- [1] Allen, M. (1987). Tildesley. dj computer simulation of liquids.
- [2] Allen, M. and Tildesley, D. (1987). Computer simulation of liquids oxford university press oxford 385.
- [3] Anderson, D., Tannehill, J. C., and Pletcher, R. H. (2016). *Computational fluid mechanics and heat transfer*. CRC Press.
- [4] Antuono, M., Colagrossi, A., and Marrone, S. (2012). Numerical diffusive terms in weakly-compressible sph schemes. *Computer Physics Communications*, 183(12):2570–2580.
- [5] Arai, M., Cheng, L.-Y., and Inoue, Y. (1994). A computing method for the analysis of water impact of arbitrary shaped bodies. *Journal of the Society of Naval Architects of Japan*, 1994(176):233–240.
- [6] Arai, M., Cheng, L.-Y., and Inoue, Y. (1995). A computing method for the analysis of water impact of arbitrary shaped bodies (2nd report). *Journal of the Society of Naval Architects of Japan*, 1995(177):91–99.
- [7] Arai, M. and Tasaki, R. (1987). A numerical study of water entrance of two-dimensional wedges. In *Proceedings of the 3rd International Symposium on Practical Design of Ships and Mobile Units, Trondheim*.
- [8] Badin, G. and Crisciani, F. (2018). *Variational Formulation of Fluid and Geophysical Fluid Dynamics*. Springer.
- [9] Batchelor, C. K. and Batchelor, G. (1967). *An introduction to fluid dynamics*. Cambridge university press.
- [10] Batchelor, G. (1974). Transport properties of two-phase materials with random structure. *Annual Review of Fluid Mechanics*, 6(1):227–255.
- [11] Batra, R. and Zhang, G. (2004). Analysis of adiabatic shear bands in elasto-thermo-viscoplastic materials by modified smoothed-particle hydrodynamics (msph) method. *Journal of computational physics*, 201(1):172–190.

- [12] Belytschko, T., Guo, Y., Kam Liu, W., and Ping Xiao, S. (2000). A unified stability analysis of meshless particle methods. *International Journal for Numerical Methods in Engineering*, 48(9):1359–1400.
- [13] Belytschko, T., Krongauz, Y., Dolbow, J., and Gerlach, C. (1998). On the completeness of meshfree particle methods. *International Journal for Numerical Methods in Engineering*, 43(5):785–819.
- [14] Belytschko, T., Krongauz, Y., Organ, D., Fleming, M., and Krysl, P. (1996). Meshless methods: an overview and recent developments. *Computer methods in applied mechanics and engineering*, 139(1-4):3–47.
- [15] Bian, X. and Ellero, M. (2014). A splitting integration scheme for the sph simulation of concentrated particle suspensions. *Computer Physics Communications*, 185(1):53–62.
- [16] Bisplinghoff, R. and Doherty, C. (1952). Some studies of the impact of vee wedges on a water surface. *Journal of the Franklin Institute*, 253(6):547–561.
- [17] Bonet, J. and Kulasegaram, S. (2000). Correction and stabilization of smooth particle hydrodynamics methods with applications in metal forming simulations. *International journal for numerical methods in engineering*, 47(6):1189–1214.
- [18] Borg, S. (1957). Some contributions to the wedge-water entry problem. *Journal of the Engineering Mechanics Division*, 83(2):1–28.
- [19] Chen, J. and Beraun, J. (2000). A generalized smoothed particle hydrodynamics method for nonlinear dynamic problems. *Computer Methods in Applied Mechanics and Engineering*, 190(1-2):225–239.
- [20] Chen, J., Beraun, J., and Carney, T. (1999). A corrective smoothed particle method for boundary value problems in heat conduction. *International Journal for Numerical Methods in Engineering*, 46(2):231–252.
- [21] Chen, J.-S., Pan, C., Wu, C.-T., and Liu, W. K. (1996). Reproducing kernel particle methods for large deformation analysis of non-linear structures. *Computer methods in applied mechanics and engineering*, 139(1-4):195–227.
- [22] Chuang, S.-L. (1969). Theoretical investigations on slamming of cone-shaped bodies. *Journal of Ship Research*.

- [23] Chuang, S.-L. et al. (1966). Experiments on flat-bottom slamming. *Journal of Ship Research*, 10(01):10–17.
- [24] Chuang, S.-L. et al. (1967). Experiments on slamming of wedge-shaped bodies. *Journal of Ship Research*, 11(03):190–198.
- [25] Chung, T. (2010). *Computational fluid dynamics*. Cambridge university press.
- [26] Cummins, S. J. and Rudman, M. (1999). An sph projection method. *Journal of computational physics*, 152(2):584–607.
- [27] Dilts, G. A. (1999). Moving-least-squares-particle hydrodynamics—i. consistency and stability. *International Journal for Numerical Methods in Engineering*, 44(8):1115–1155.
- [28] Dilts, G. A. (2000). Moving least-squares particle hydrodynamics ii: conservation and boundaries. *International Journal for Numerical Methods in Engineering*, 48(10):1503–1524.
- [29] Dobrovol’skaya, Z. (1969). On some problems of similarity flow of fluid with a free surface. *Journal of Fluid Mechanics*, 36(4):805–829.
- [30] Dyka, C. and Ingel, R. (1995). An approach for tension instability in smoothed particle hydrodynamics (sph). *Computers & structures*, 57(4):573–580.
- [31] Dyka, C., Randles, P., and Ingel, R. (1997). Stress points for tension instability in sph. *International Journal for Numerical Methods in Engineering*, 40(13):2325–2341.
- [32] Eriksson, J. (2018). Evaluation of sph for hydrodynamic modeling, using dual-sphysics.
- [33] Fang, J., Owens, R. G., Tacher, L., and Parriaux, A. (2006). A numerical study of the sph method for simulating transient viscoelastic free surface flows. *Journal of Non-Newtonian Fluid Mechanics*, 139(1-2):68–84.
- [34] Fang, J. and Parriaux, A. (2008). A regularized lagrangian finite point method for the simulation of incompressible viscous flows. *Journal of Computational physics*, 227(20):8894–8908.
- [35] Fang, J., Parriaux, A., Rentschler, M., and Ancy, C. (2009). Improved sph methods for simulating free surface flows of viscous fluids. *Applied Numerical Mathematics*, 59(2):251–271.

- [36] Frenkel, D. and Smit, B. (2001). *Understanding molecular simulation: from algorithms to applications*, volume 1. Elsevier.
- [37] Fulk, D. A. and Quinn, D. W. (1996). An analysis of 1-d smoothed particle hydrodynamics kernels. *Journal of Computational Physics*, 126(1):165–180.
- [38] Garabedian, P. (1953). Oblique water entry of a wedge. *Communications on Pure and Applied Mathematics*, 6(2):157–165.
- [39] Gingold, R. and Monaghan, J. (1982). Kernel estimates as a basis for general particle methods in hydrodynamics. *Journal of Computational Physics*, 46(3):429–453.
- [40] Gingold, R. A. and Monaghan, J. J. (1977). Smoothed particle hydrodynamics: theory and application to non-spherical stars. *Monthly notices of the royal astronomical society*, 181(3):375–389.
- [41] GR, L. (2003). *Smoothed particle hydrodynamics*. Number BOOK. Singapore, World Scientific Publishing Co. Pte. Ltd, 2003.
- [42] Greenhow, M. (1987). Wedge entry into initially calm water. *Applied Ocean Research*, 9(4):214–223.
- [43] Greenhow, M. and Lin, W.-M. (1983). Nonlinear-free surface effects: experiments and theory. Technical report, Massachusetts Inst Of Tech Cambridge Dept Of Ocean Engineering.
- [44] Groot, R. D. and Warren, P. B. (1997). Dissipative particle dynamics: Bridging the gap between atomistic and mesoscopic simulation. *The Journal of chemical physics*, 107(11):4423–4435.
- [45] Gui-rong, L. (2003). *Smoothed Particle Hydrodynamics: A Meshfree Particle Method*. World Scientific Publishing Company.
- [46] Hashemi, M., Fatehi, R., and Manzari, M. (2012). A modified sph method for simulating motion of rigid bodies in newtonian fluid flows. *International Journal of Non-Linear Mechanics*, 47(6):626–638.
- [47] Hieber, S. E. and Koumoutsakos, P. (2008). An immersed boundary method for smoothed particle hydrodynamics of self-propelled swimmers. *Journal of Computational Physics*, 227(19):8636–8654.

- [48] Hockney, R. W. and Eastwood, J. W. (1988). *Computer simulation using particles*. crc Press.
- [49] Hoogerbrugge, P. and Koelman, J. (1992). Simulating microscopic hydrodynamic phenomena with dissipative particle dynamics. *EPL (Europhysics Letters)*, 19(3):155.
- [50] Hu, X. and Adams, N. (2006). Angular-momentum conservative smoothed particle dynamics for incompressible viscous flows. *Physics of Fluids*, 18(10):101702.
- [51] Johnson, G. R. (1996). Artificial viscosity effects for sph impact computations. *International Journal of Impact Engineering*, 18(5):477–488.
- [52] Johnson, G. R. and Beissel, S. R. (1996). Normalized smoothing functions for sph impact computations. *International Journal for Numerical Methods in Engineering*, 39(16):2725–2741.
- [53] Kleefsman, K., Fekken, G., Veldman, A., Iwanowski, B., and Buchner, B. (2005). A volume-of-fluid based simulation method for wave impact problems. *Journal of computational physics*, 206(1):363–393.
- [54] Kolukisa, D., Özbulut, M., and Peşman, E. (2017). An investigation on the effects of time integration schemes on weakly compressible sph method.
- [55] Koshizuka, S., Nobe, A., and Oka, Y. (1998). Numerical analysis of breaking waves using the moving particle semi-implicit method. *International Journal for Numerical Methods in Fluids*, 26(7):751–769.
- [56] Kozlov, I. M., Dobrego, K. V., and Gnesdilov, N. N. (2011). Application of res methods for computation of hydrodynamic flows by an example of a 2d flow past a circular cylinder for $re= 5-200$. *International Journal of Heat and Mass Transfer*, 54(4):887–893.
- [57] Lee, E.-S., Moulinec, C., Xu, R., Violeau, D., Laurence, D., and Stansby, P. (2008). Comparisons of weakly compressible and truly incompressible algorithms for the sph mesh free particle method. *Journal of computational Physics*, 227(18):8417–8436.
- [58] Li, S. and Liu, W. K. (2002). Meshfree and particle methods and their applications. *Applied Mechanics Reviews*, 55(1):1–34.
- [59] Liu, G. (2002). *Mesh free methods: moving beyond the finite element method*. CRC press.

- [60] Liu, G., Zhang, J., Lam, K., Li, H., Xu, G., Zhong, Z., Li, G., and Han, X. (2008). A gradient smoothing method (gsm) with directional correction for solid mechanics problems. *Computational Mechanics*, 41(3):457–472.
- [61] Liu, G.-R. and Gu, Y.-T. (2005). *An introduction to meshfree methods and their programming*. Springer Science & Business Media.
- [62] Liu, M. and Liu, G. (2010). Smoothed particle hydrodynamics (sph): an overview and recent developments. *Archives of computational methods in engineering*, 17(1):25–76.
- [63] Liu, M., Liu, G., and Lam, K. (2003a). Constructing smoothing functions in smoothed particle hydrodynamics with applications. *Journal of Computational and applied Mathematics*, 155(2):263–284.
- [64] Liu, M., Liu, G., and Lam, K. (2003b). A one-dimensional meshfree particle formulation for simulating shock waves. *Shock Waves*, 13(3):201–211.
- [65] Liu, M., Liu, G., Lam, K., and Zong, Z. (2003c). Smoothed particle hydrodynamics for numerical simulation of underwater explosion. *Computational Mechanics*, 30(2):106–118.
- [66] Liu, M. and Liu, G.-R. (2006). Restoring particle consistency in smoothed particle hydrodynamics. *Applied numerical mathematics*, 56(1):19–36.
- [67] Liu, M., Shao, J., and Li, H. (2014). An sph model for free surface flows with moving rigid objects. *International Journal for Numerical Methods in Fluids*, 74(9):684–697.
- [68] Liu, M., Xie, W., and Liu, G. (2005). Modeling incompressible flows using a finite particle method. *Applied mathematical modelling*, 29(12):1252–1270.
- [69] Liu, W. K., Chen, Y., Jun, S., Chen, J., Belytschko, T., Pan, C., Uras, R., and Chang, C. (1996). Overview and applications of the reproducing kernel particle methods. *Archives of Computational Methods in Engineering*, 3(1):3–80.
- [70] Lucy, L. B. (1977). A numerical approach to the testing of the fission hypothesis. *The astronomical journal*, 82:1013–1024.
- [71] Marrone, S., Colagrossi, A., Antuono, M., Colicchio, G., and Graziani, G. (2013). An accurate sph modeling of viscous flows around bodies at low and moderate reynolds numbers. *Journal of Computational Physics*, 245:456–475.

- [72] Meringolo, D. D., Aristodemo, F., and Veltri, P. (2015). Sph numerical modeling of wave-perforated breakwater interaction. *Coastal Engineering*, 101:48–68.
- [73] Monaghan, J. (1985). Particle methods for hydrodynamics. *Computer Physics Reports*, 3(2):71 – 124.
- [74] Monaghan, J. (1994). Simulating free surface flows with sph. *Journal of computational physics*, 110(2):399–406.
- [75] Monaghan, J. and Kos, A. (1999). Solitary waves on a cretan beach. *Journal of waterway, port, coastal, and ocean engineering*, 125(3):145–155.
- [76] Monaghan, J. J. (1982). Why particle methods work. *SIAM Journal on Scientific and Statistical Computing*, 3(4):422–433.
- [77] Monaghan, J. J. (1992). Smoothed particle hydrodynamics. *Annual review of astronomy and astrophysics*, 30(1):543–574.
- [78] Monaghan, J. J. and Lattanzio, J. C. (1985). A refined particle method for astrophysical problems. *Astronomy and astrophysics*, 149:135–143.
- [79] Morris, J. P. (1996). *Analysis of smoothed particle hydrodynamics with applications*. Monash University Australia.
- [80] Nguyen, V. P., Rabczuk, T., Bordas, S., and Dufloy, M. (2008). Meshless methods: a review and computer implementation aspects. *Mathematics and computers in simulation*, 79(3):763–813.
- [81] Oger, G., Doring, M., Alessandrini, B., and Ferrant, P. (2006). Two-dimensional sph simulations of wedge water entries. *Journal of computational physics*, 213(2):803–822.
- [82] Özbulut, M., Tofghi, N., Gören, Ö., and Yıldız, M. (2015). On the sph modelling of flow over cylinder beneath to a free-surface.
- [83] Ozbulut, M., Tofghi, N., Goren, O., and Yildiz, M. (2018). Investigation of wave characteristics in oscillatory motion of partially filled rectangular tanks. *Journal of Fluids Engineering*, 140(4):041204.
- [84] Ozbulut, M., Yildiz, M., and Goren, O. (2014). A numerical investigation into the correction algorithms for sph method in modeling violent free surface flows. *International Journal of Mechanical Sciences*, 79:56–65.

- [85] Pakozdi, C. (2008). A smoothed particle hydrodynamics study of two-dimensional nonlinear sloshing in rectangular tanks. *Department of Marine Technology. Trondheim, Norwegian University of Science and Technology. Doctoral Thesis.*
- [86] Payne, P. R. (1981). The vertical impact of a wedge on a fluid. *Ocean Engineering*, 8(4):421–436.
- [87] Rabczuk, T., Belytschko, T., and Xiao, S. (2004). Stable particle methods based on lagrangian kernels. *Computer methods in applied mechanics and engineering*, 193(12-14):1035–1063.
- [88] Randles, P. and Libersky, L. (2000). Normalized sph with stress points. *International Journal for Numerical Methods in Engineering*, 48(10):1445–1462.
- [89] Randles, P. and Libersky, L. D. (1996). Smoothed particle hydrodynamics: some recent improvements and applications. *Computer methods in applied mechanics and engineering*, 139(1-4):375–408.
- [90] Shadloo, M. S., Zainali, A., Yildiz, M., and Suleman, A. (2012). A robust weakly compressible sph method and its comparison with an incompressible sph. *International Journal for Numerical Methods in Engineering*, 89(8):939–956.
- [91] Shao, S. (2009). Incompressible sph simulation of water entry of a free-falling object. *International Journal for numerical methods in fluids*, 59(1):91–115.
- [92] Siegel, S., Fagley, C., and Nowlin, S. (2012). Experimental wave termination in a 2d wave tunnel using a cycloidal wave energy converter. *Applied Ocean Research*, 38:92–99.
- [93] Sigalotti, L. D. G., Klapp, J., Sira, E., Meleán, Y., and Hasmy, A. (2003). Sph simulations of time-dependent poiseuille flow at low reynolds numbers. *Journal of computational physics*, 191(2):622–638.
- [94] Sweigle, J., Hicks, D., and Attaway, S. (1995). Smoothed particle hydrodynamics stability analysis. *Journal of computational physics*, 116(1):123–134.
- [95] Tasai, F. (1960). Damping force and added mass of ships heaving and pitching (continued). *Reports of Research Institute for Applied Mechanics*, (31).
- [96] Tofighi, N., Ozbulut, M., Rahmat, A., Feng, J. J., and Yildiz, M. (2015). An incompressible smoothed particle hydrodynamics method for the motion of rigid bodies in fluids. *Journal of Computational Physics*, 297:207–220.

- [97] Vignjevic, R., Campbell, J., and Libersky, L. (2000). A treatment of zero-energy modes in the smoothed particle hydrodynamics method. *Computer methods in Applied mechanics and Engineering*, 184(1):67–85.
- [98] Vinje, T. and Brevig, P. (1980). Nonlinear two-dimensional ship motions. *In Proceedings of the 3rd International Conference on Numerical Ship Hydrodynamics. Paris, France.*
- [99] Von Karman, T. (1929). The impact on seaplane floats during landing.
- [100] Wagner, H. (1932). The phenomena of impacts and sliding on liquid surfaces.
- [101] XG, X. and GR, L. (2008). *An adaptive gradient smoothing method (GSM) for fluid dynamics problems.* Int J Numer Methods Fluids.
- [102] XG, X., GR, L., and KH, L. (2009). *Application of gradient smoothing method (GSM) for steady and unsteady incompressible flow problems using irregular triangles.* Int J Numer Methods Fluids (submitted).
- [103] Yettou, E.-M., Desrochers, A., and Champoux, Y. (2006). Experimental study on the water impact of a symmetrical wedge. *Fluid Dynamics Research*, 38(1):47.
- [104] Zhang, G. and Batra, R. (2004). Modified smoothed particle hydrodynamics method and its application to transient problems. *Computational mechanics*, 34(2):137–146.
- [105] Zhang, S. et al. (1976). Detonation and its applications. *Press of National Defense Industry, Beijing.*
- [106] Zhang, Y., Zou, Q., Greaves, D., Reeve, D., Hunt-Raby, A., Graham, D., James, P., and Lv, X. (2010). A level set immersed boundary method for water entry and exit. *Communications in Computational Physics*, 8(2):265–288.
- [107] Zhao, R. and Faltinsen, O. (1993). Water entry of two-dimensional bodies. *Journal of Fluid Mechanics*, 246:593–612.
- [108] Zhirong, S., Yi-Fang, H., Zhongfu, G., Richard, K., James, H., and of Shipping, A. B. (2016). *Slamming Load Prediction Using Overset CFD Methods.* Offshore Technology Conference.
- [109] Zienkiewicz, O. and Taylor, R. (2000). The finite element method, butterworth heinemann.